國立交通大學

土木工程研究所

碩士論文

滲出水集排特性對掩埋場邊坡穩定度之影響

Leachate Water Balance and Its Effect on Slope Stability of Landfill

研　究　生：盧彥森

指導教授：單信瑜　　博士

中華民國九十九年二月

滲出水集排特性對掩埋場邊坡穩定度之影響

研究生：盧彥森　　指導教授：單信瑜博士

國立交通大學土木工程研究所

摘要

由於台灣地狹人稠，土地取得不易，導至許多掩埋場座落於山谷之間。當掩埋場位於山區間時，由於滲出水水頭高的上升，或是掩埋場底部的地工合成材因過濕潤，較易發生邊坡滑移破壞的情況，造成掩埋場的破壞，甚至是人命的損失。因此本研究將藉由水文平衡分析軟體 HELP (Hydrologic Evaluation of Landfill Performance)探討掩埋場中滲出水集排系統對滲出水的效能，並以邊坡穩定分析軟體 SLOPE/W 對掩埋場的穩定性做分析，探討滲出水水頭高對掩埋場穩定性之影響。在此研究中，為針對台灣北、中、南部三地區的掩埋場做分析，其中選擇了八里掩埋場、頭份掩埋場與安定掩埋場為本研究之對象。研究結果顯示，滲出水水頭高主要在滲出水集排系統的劣化下升高，而廢棄物滲透係數的上升，將造成滲出水延遲收集時間的增加。由邊坡穩定分析得知，安全係數會因為滲出水水頭高的增加、掩埋場襯砌層間介面摩擦角的降低與掩埋場高度的增加而下降，另一方面，介面襯砌層間介面摩擦角的下降，對掩埋場穩定性最為影響。

A Study of Leachate Waste Balance and Its Effect on Slope Stability of Landfill

By

Student: Yen-Sen Lu Advisor: Dr. Hsin-Yu Shan

Department of Civil Engineering

National Chiao Tung University

Abstract

Many of the landfills in Taiwan are located in the valleys or mountain areas due to the shortage of land. Meanwhile, the valley-filled landfill will face the slope failure which is caused by the buildup of leachate. Hence, the clogging Leachate Collection and Removal System (LCRS) might cause the instability of landfill slopes. The objective of this study is to simulate the performance of LCRS by Visual HELP (Hydrologic Evaluation of Landfill Performance) and evaluate the slope stability by SLOPE/W. In order to study landfills in northern, central, and southern Taiwan, Bali Landfill, Toufen Landfill, and Anding Landfill are selected respectively. The results show that the leachate head will rise due to the degradation of the LCRS. In addition, the decrease of hydraulic conductivity of the waste layer will increase the time lag of leachate collection. As indicated by the result of slope stability analysis, the factor of safety will decrease with the increase of the height of waste, increases of the leachate head, and the decrease of the interfacial friction angle of liner system. Moreover, the interfacial friction angle of liner system is most critical to the stability of the landfill.

Keywords: landfill, leachate collection and removal system, slope stability, HELP

謝誌

算一算，在交大也待了六年多了，也同時讓單信瑜老師照顧了六年，實在是很感謝老師指導與關心，讓我的六年來的校園生活畫上一筆色彩繽紛。研究上也很感謝徐松圻老師、賴俊仁老師、劉家男老師的細心指教，讓我受益良多，也感謝陳宏益科長的大力支持與幫助，才使得我的研究能夠有著美好的結果。

研究所期間當然更不能忘了大地組的夥伴們，尤其是同實驗室的培旼、韋恩、凱仁、韋甫，能夠與大家相識相遇，真的是很令人開心的事。當然別忘了溫柔嫻熟的系辦小姐們。

最後一定是要感謝家人的支持與相伴，沒有他們，也就不會有今日的我，當然還有可愛的未婚妻雯妃，與長得很像西鄉隆盛前室友敬程，是我人生路上最重要的兩人，也是我心靈上最大的依靠。最後的最後一定要提一下林明璋實驗室的朋友，希望有一天能再一起去爬山吧！

Contents

Figures List

Table List

Chapter 1 Introduction

1.1 Background

Due to the difficulty of obtaining land for disposing the municipal solid wastes or incinerator ash, many municipal solid waste landfills in Taiwan are located in mountain areas. Liner system is installed in the landfill to collect the leachate for treatment and prevent the leakage of leachate. Many reported slope failure of landfills have been associated with the excessive buildup of leachate level and excessive wetness of the geosynthetic interface, both of which is in turn related to clogging Leachate Collection and Removal Systems (LCRS).

The buildup of leachate head in the landfill will cause the failure but the importance of avoiding clogging of LCRS is sometimes ignored. Moreover, the leachate production rate and the ponding leachate head on the liner system is seldom monitored in Taiwan's landfill. Moreover, due to the error design and lack of maintenance, some landfills have to face the problem of LCRS clogging. In Taiwan, the regulation does not emphasize on the design of LCRS hence the performance of LCRS is doubtable. In addition, the design of LCRS does not fully employ the water balance simulation. Thus, the performance of LCRS should be examined and the design of LCRS should be improved.

1.2 Research Objectives

The objective of this study is to understand the performance of LCRS in various situations by simulating real landfills for water balance analysis and slope stability analysis. Three sites of landfill are located in the south, central, and north of Taiwan. They are chosen to be analyzed because of the different rainfall intensity, type of landform, and types of waste. In each landfill, different slope of LCRS and material

parameters are applied to water balance calculation. The results of leachate head are then used for slope stability analysis to study the consequential effect.

Chapter 2 Literature Review

2.1 Landfill Design and Operation

The major components of landfill are the liner system and the cover system. The liner system consists of LCRS and hydraulic barrier system. A typical profile of landfill is shown in Figure 2-1. The LCRS will drain the leachate out of the landfill to the wastewater treatment plant. The hydraulic barrier system will prevent leachate from infiltrating into the ground underneath the landfill. The gas produced by the waste will be collected with the gas collection system. When the waste reaches the designed volume, the cover system will be constructed to reduce the generation of leachate and the landfill will be closed.

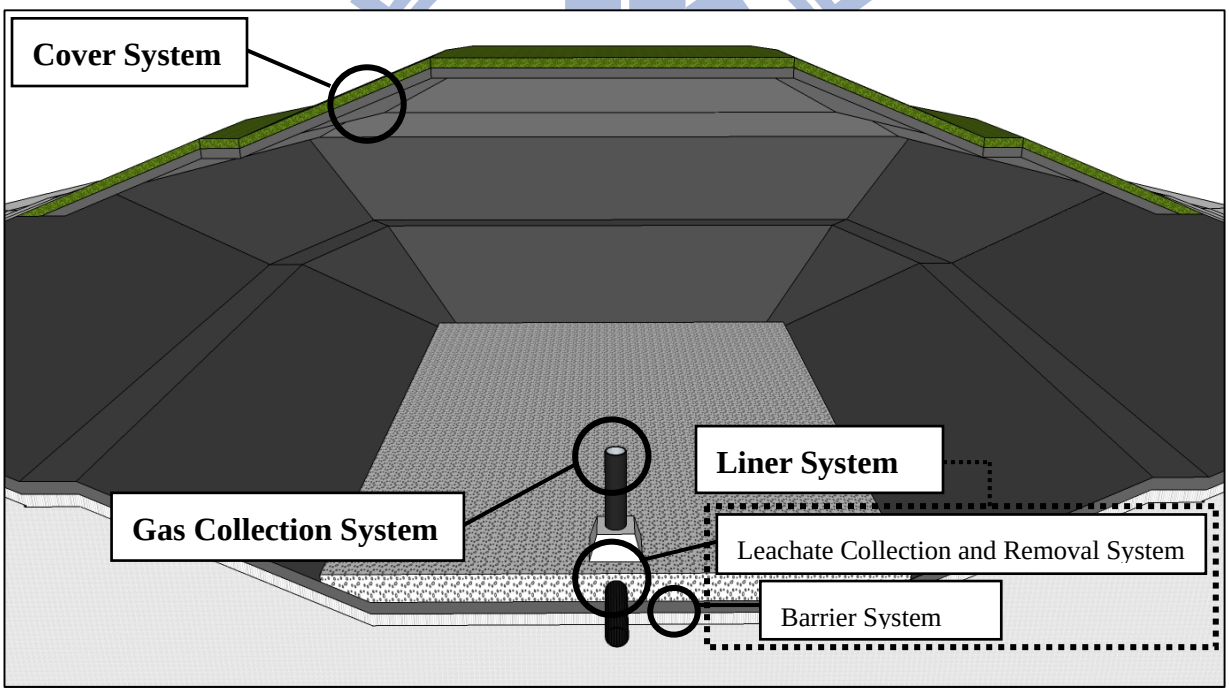

Figure 2-1: 3D Profile of the Landfill

2.2 Slope Stability Issue

Landfill is categorized into four types by the mode of fill, including area fill, trench fill, above and below ground fill, and valley fill (Qian et al., 2001). The waste in

valley-filled landfill is piled from the bottom of landfill and the shape of the waste layer tends to be parallelogram as shown in Figure 2-2.

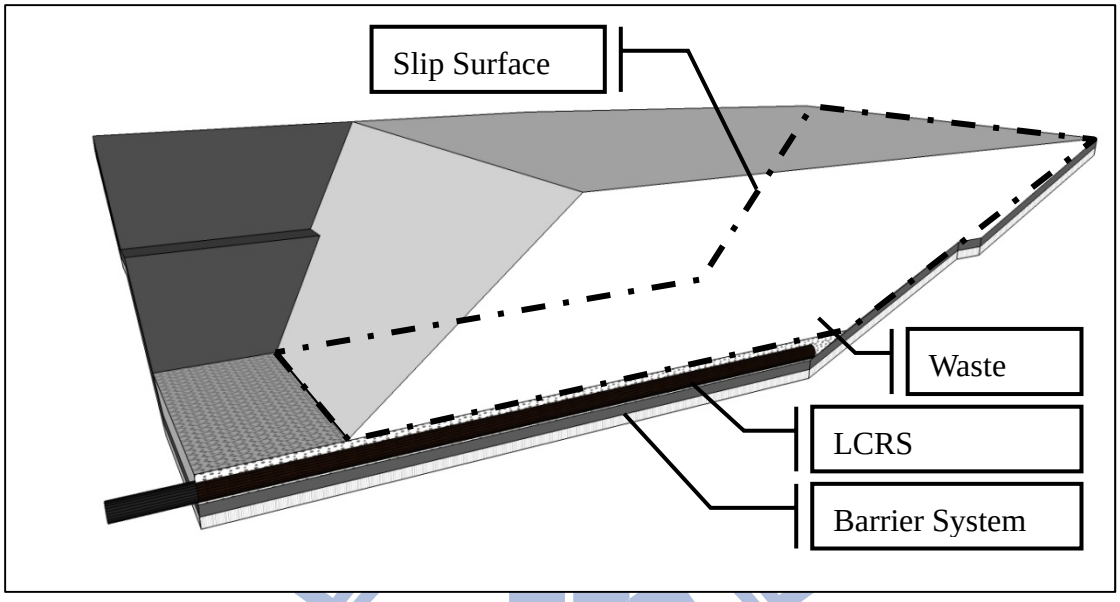

Figure 2-2: Profile of Valley-filled Landfill During Operation

The slope stability is critical to landfills in mountain areas. As indicated in Table 2-1, most landfills installed with liner system are involved with translational failure. The translational failure of landfill is due to two main mechanisms, including buildup of leachate head and wetting of interface in liner system (Qian and Koerner, 2005). The slip surface of translational failure lies along the liner system due to the low interfacial strength. Furthermore, absorption of leachate will cause of the increasing of unit weight of waste and thus will lower the stability of the waste (Koerner and Soong, 2000).

2.2.1 Interface Strength of Geosynthetics

There have been many studies on the interfacial shear strength between the geosynthetics or between soil and geosynthetics (Liu, 2004). In a series of shear strength test for interfaces of HDPE geomembrane and clay, the residual shear strength is about

43.1 kPa in submerged interface condition (Mitchell and Seed, 1990). The interfacial shear strength of HDPE geomembrane/compacted clay is between 11° and 14° while the clay is compacted to field density and water content. The unit weight of waste is17.3 kN/m^3 and the height of overlying waste-fill is approximately 17.7 m, hence the residual friction angle can be determined as 8° (Seed and Mitchell, 1990). Some suggest that the friction angle of interface between geosynthestics should be as low as 8°. In the meantime, HDPE geomembrane and saturated compacted clay may be low while being in wet condition (Mitchell and Mitchell, 1992).

In the field test of slope stability for geosynthetic clay liner (GCL), the interface strength may be low since the bentonite inside the GCL tends to extrude through the opening of the geotextiles as GCL hydrates and thus reduce the interfacial shear strength (Daniel et al., 1998). The interfacial shear strength obtained from the laboratory tests on the shear strength of the HDPE geomembrane and GCL interface are listed in Table 2-2 (Triplett and Fox, 2001). For smooth HDPE geomembrane/hydrated GCL interface, the residual cohesion is between 0.3 kPa and 5.8 kPa, and the friction angle is between 6.9° and 9.2°, respectively.

2.2.2 Properties of Municipal Solid Waste

The unit weight and strength parameters of municipal solid waste (MSW) are listed in Table 2-3. The unit weight ranges from 2.9 kN/m^3 to 14.4 kN/m^3. For shear strength parameters, the cohesion ranges from 0 kPa to 67 kPa, and the friction angle covers from 9.2° to 53° due to the high heterogeneity of MSW.

The results of several researches on hydraulic properties of MSW are summarized in Table 2-4. The range of hydraulic conductivity of waste is from 4.0×10^{-2} cm/s to 4.2×10^{-5} cm/s.

Table 2-1: Summary of Landfill Failure (Qian and Koerner, 2005)

Case No	Type of Failure	Reason for Low Initial FS	Triggering Mechanism
U-3	Translational	Leachate Buildup Within Waste Mass	Excessive buildup of leachate level due to ponding
U-4			Excessive buildup of leachate level due to ice formation
L-4			Excessive buildup of leachate level due to liquid waste
L-5			Excessive buildup of leachate level due to leachate injection
L-6			Excessive buildup of leachate level due to closed outlet valve
L-7			Excessive buildup of leachate level due to leachate injection
U-7	Single Rotational		Excessive buildup of leachate level due to heavy rains (hurricane)
L-1	Translational	Wet Clay Beneath GM,i.e. GM/CCL composite	Excessive wetness of the GM/CCL interface
L-2			Excessive wetness of the GM/CCL interface
L-3			Excessive wetness of the bentonite in an unreinforced GCL
U-1	Single Rotational	Wet Foundation or Soft Backfill Soil	Rapid rise in leachate level within the waste mass
U-5			Excessive buildup of perched leachate level on clay liner
U-6			Progressively weaker foundation soils
U-2	Multiple Rotational		Foundation soil excavation exposing soft clay

L: LINER

U: UNLINER

Table 2-2: Summary of HDPE/GCL Interfacial Shear Strength (Triplett and Fox, 2001)

GM/GCL Interface	Normal Stress range (kPa)	Peak Strengh		Normal Stress range (kPa)	Large Displacement (200 mm)	
		Cohesion (kPa)	Friction Angle (°)		Cohesion (kPa)	Friction Angle (°)
SM/W	6.9-486	0.3	9.8	6.9-127	0.3	8.1
				127-486	3.0	6.9
SM/NW	6.9-486	0.4	9.9	6.9-127	0.6	9.2
				127-486	5.8	6.9

SM/W: 40 mil smooth HDPE / Woven geotextiles of woven/nonwoven needle-punched GCL

SM/NW: 40 mil smooth HDPE / Nonwoven geotextiles of woven/nonwoven needle-punched GCL

Table 2-3: Unit Weight and Strength Parameters of Municipal Solid Waste

Unit weight (kN/m^3)	Shear Strength Parameters		Method	Reference
	Cohesion (kPa)	Friction Angle (°)		
7 - 14	0 - 23	24 - 41	In-situ/Lab Test	(Landva and Clark, 1990)
2.9 - 14.4	0 - 67	10 - 53	Summary	(Kavazanjian et al., 1995)
3.0 - 10.5	0 - 28	15 - 42	Summary	(Dixon and Jones, 2005)
5.9 - 9.8	0 - 5.8	9.2 - 46.2	Lab Test	(ZHENG, 2004)
4.41 - 7.36	33.6 - 34.9	32.1 - 38.0	In-situ Test	(Fan and Shan, 2007)

Table 2-4: Hydraulic Properties of Municipal Solid Waste

Hydraulic Conductivity (cm/s)	Field Capacity (vol/vol)	Wilting Point (vol/vol)	Initial Water Content (%)	Method	Reference
1.0×10^{-2} - 1.0×10^{-4}	5.8-9.2		8.55 - 20.5	Lysimeter	(Fungaroli and Steiner, 1979)
4.0×10^{-2} - 1.0×10^{-3}				Percolation test in pits	(Landva and Clark, 1990)
1.0×10^{-3}- 1.5×10^{-4}	0.35	0.20	10 - 20	Pumping Test	(Oweis et al., 1990)
	0.12	0.11	18.4 - 6.7	ASTM 2325	(Benson and Wang, 1998)
1.1×10^{-3} - 2.9×10^{-4}	0.36	0.17	39.0	Lab test	(Jang et al., 2002)

2.3 Leachate Collection and Removal System

2.3.1 Design and Hydraulic Properties of LCRS

Leachate is generated from the initial water content of the waste, precipitation, and the degradation of wastes. In order to prevent the buildup of leachate head, LCRS is installed to collect the leachate from treatment. An LCRS is composed of a drainage blanket and a system of drainage pipes. Drainage pipes are placed in a fishbone pattern in the landfill and wrapped by gravel and geotextiles (Figure 2-3). The geotextiles is

used for protecting the drainage system from the clogging by the fines of waste or soil. The landfill which stores hazardous waste will have more than one leachate collection system. Therefore a secondary drainage layer will be installed underneath in order to detect the leakage of leachate.

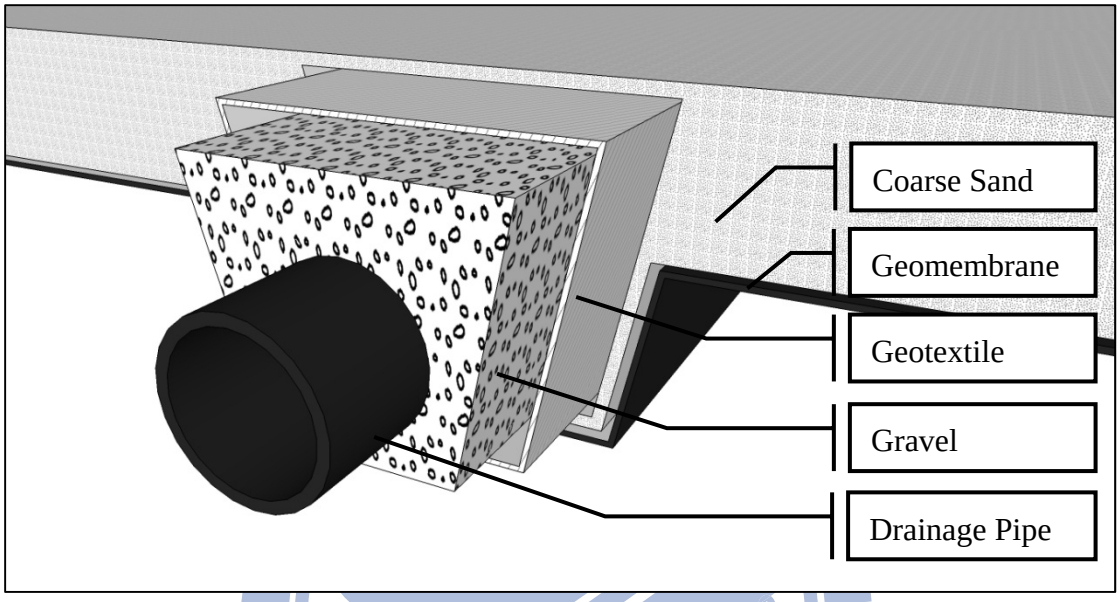

Figure 2-3: Profile of Leachate Collection and Removal System

2.3.2 Design of LCRS

According to the regulation of landfill by of Taiwan (Department of Health, 1985), the basic liner system should consist of a drainage pipe with 1 m/s flow rate and a barrier with at least 10^{-6} cm/s of hydraulic conductivity. U.S Environmental Protection Agency (USEPA) demands that the leachate head should be less than 30 cm (or 1 ft). In addition, there is no demand for specific flow rate of LCRS but the drainage layer shall be designed to reduce the leachate head on the liner system generated by the 24-hours, 2-year storm in 72 hours after the storm (USEPA, 1992).

For the prediction of leachate production in Taiwan, the rational method (Kuich-ling, 1889):

$$Q=\frac{1}{1000}C\cdot I\cdot A \quad \text{.....(2.1)}$$

is used, where Q is the peak discharge (m^3); C is the runoff coefficient; I is the rainfall intensity (mm/hr); A is the drainage area (m^2). Based on Equation 2.1, some equation for predicting leachate production is developed and applied (Wang, 2007). The modified rational method (Foundation Conference on National Urban Cleaning, 1989):

$$Q=\frac{1}{1000}(C_1\cdot A_1+C_2\cdot A_2)\cdot I \quad \text{.....(2.2)}$$

where the C_1 is the runoff coefficient for the area of few-runoff and operation; C_2 is the runoff coefficient for the area of mass-runoff and closed area; A_1 the area of few-runoff and operation; A_2 is the area of mass-runoff and closed area, is often used.

2.3.3 Clogging of Leachate Collection and Removal System

Researches indicate that the LCRS might clog in different situations. The majority of clogging of LCRS can be classified as three types: biological, physical, and chemical (Rowe and VanGulck, 2004). Field observations show that a thick slime layer was observed in the drainage blanket layer and the drainage pipe was clogged by the mineral deposit (Fleming et al., 1999). In another field study, the hydraulic conductivity of sand was found to reduce from 4.3×10^{-2} cm/s to 1.6×10^{-5} cm/s because of the cementing within the void of the sand (Koerner and Koerner, 1995a).

The leachate of waste provides substance and nutrition for bacteria and hence the growing of biofilm inside the geotextiles induces the clogging (Mlynarek and Rollin, 1995). In laboratory tests on clogging by biofilm, the permeability of geotextiles was shown to decrease from 10^{-2} cm/s to 9.0×10^{-5} cm/s (Koerner and Koerner, 1995b) and 4×10^{-1} cm/s to 9×10^{-4} cm/s (Palmeira et al., 2008). On the other hand, the geotextiles soaked in the leachate are clogged by organic material and fine sediment. The permeability of geotextiles was observed in the field and was found to decrease from 2.3×10^{-1} cm/s to 7.5×10^{-5} cm/s (Koerner and Koerner, 1995a).

2.4 Water Balance Calculation: Hydrologic Evaluation of Landfill Performance

Hydrologic Evaluation of Landfill Performance (HELP) is the most widely used computer program for water balance analysis of landfill (Albright et al., 2002; Nixon et al., 1997). HELP is developed by U.S. Army Engineer Waterways Experiment Station for the USEPA (Schroeder et al., 1994a). HELP is a quasi-two-dimensional hydrologic model of water movement into or out from landfill, hence the calculation is one-dimensioned (Schroeder et al., 1994b). HELP have been used widely in the U.S.A for the design of landfill. In other countries, HELP was also employed in some studies and the results are fairly close to field data (Dho et al., 2002; Jang et al., 2002; Klaus, 2000).

2.4.1 Calculation Methods of HELP Model

The procedure of HELP can be described as six parts: weather input, and computation of runoff, potential evaporation, vertical drainage, lateral drainage, and geomembrane leakage (Schroeder et al., 1994b):

1. Weather Data: Weather data can be input by historical data or generated by weather generator. The weather data used in HELP includes precipitation, temperature, solar radiation, wind speed, and relative humidity.
2. Runoff Computation: SCS curve-number method is used for runoff. The adjustment of curve number is related to the various levels of vegetation and the soil types in HELP model (USDA, 1985).
3. Evaporation Computation: The method follows the approach recommended by Ritchie (1972). Besides, a modified Penman (1963) equation

$$ES_{0i} = \frac{(PENR_i + K_{Ei} PENA_i) \times e^{(10.000029 CV_i)}}{25.4 \times (59.7 - 0.0564 T_{ci})} \quad \text{.....(2.3)}$$

is used for soil water evaporation. This part contains potential evapotranspiration, surface evaporation, soil water evaporation, and plant transpiration.

4. Vertical Drainage Computation: The governing equation for vertical drainage is Darcy's law which will calculate the rate of vertical flow. In addition, Compell's equation (1974),

$$K = K_s\left(\frac{SM-RS}{UL-RS}\right)^{3+\frac{2}{\lambda}} \quad \text{.....(2.4)}$$

is applied to the unsaturated hydraulic conductivity.

5. Lateral Drainage Computation: The lateral drainage is considered as a flow in unconfined porous media and hence the Boussinesq equation (1904)

$$\int \frac{\partial h}{\partial t} = K_D \frac{\partial}{\partial l}\left[(h - l\sin\alpha)\frac{\partial h}{\partial l}\right] + R, \quad \text{.....(2.5)}$$

is used for calculation. The percentage of lateral drainage is able to add to one layer for recirculation.

6. Geomembrane Leakage Computation: The calculation for leakage is based on Giroud and Bonaparte's procedures. It will take area of defects, punctures, tears, cracks and seam situation into calculation (Giroud and Bonaparte, 1989).

2.4.2 Limitation of HELP

According to the researches on HELP, some limitations were mentioned. The parameters of surface and cover materials are found to affect the runoff, evapotranspiration mostly. The under-predicted lateral drainage and runoff are due to the over-estimation of the hydraulic conductivity of surface layers, which decrease the infiltration of the precipitation. Moreover, the leachate production is under the influence of the evaporative depth. While the evaporative depth increases from 10 cm to 46 cm,

the leachate production decreases by more than 50% (Payton and Schroeder, 1988).

In additional, HELP cannot calculate while the waste layer or LCRS degrades. Furthermore, HELP neglects the aging of cover system (Berger et al., 1996; Klaus, 2000). The HELP does not incorporate the degradation of specific layer, and should be supervised carefully during the construction. In this research, HELP is stated as simple because of the empirical modeling approach. In the other hand, there are more than a hundred empirical or theoretical equations for different situation and layer. Therefore, HELP is defined as very complex due to the different description of hydrological process.

Chapter 3 Research Methodology

3.1 Structure of the Research Program

The structure of this study is shown in the flow chart in Figure 3-1. Visual HELP is developed for the Windows interface of HELP which was originally developed on DOS. Thus the latest version of Visual HELP is employed in this study.

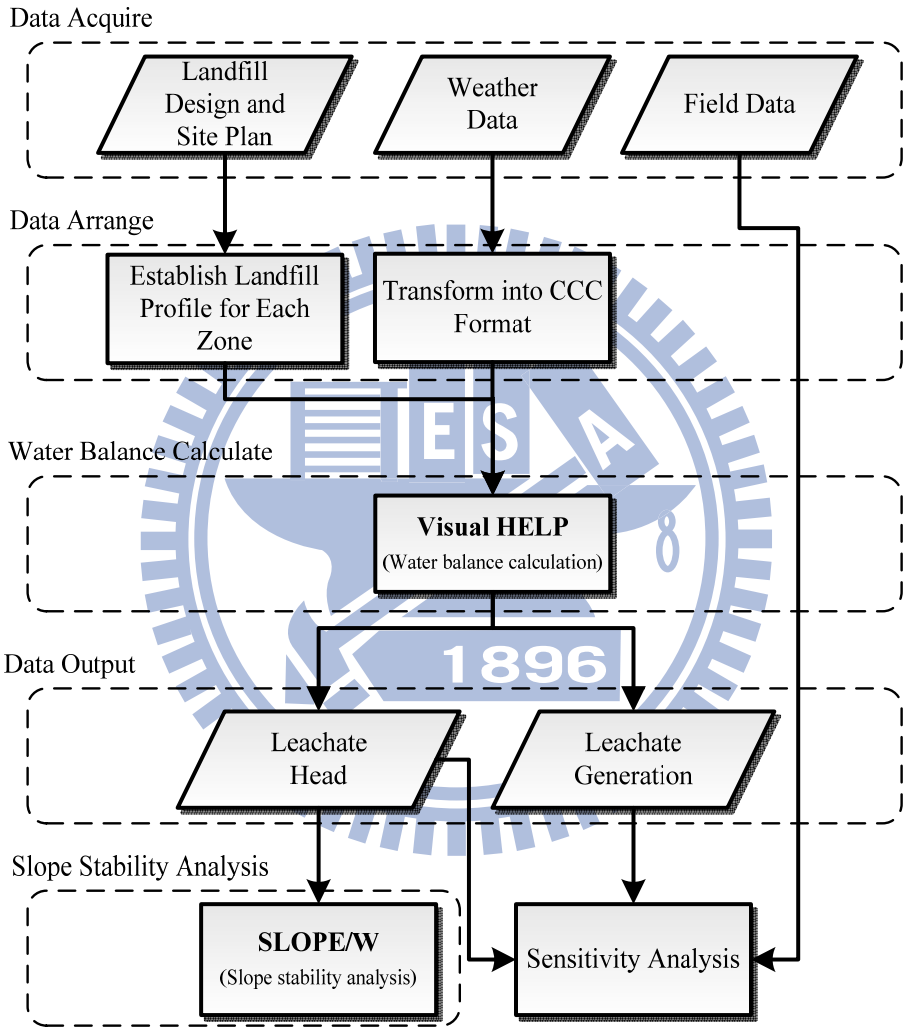

Figure 3-1: Analysis flow chart

The weather data obtained from Central Weather Bureau is in the form of date-value which is unacceptable by Visual HELP. Hence, the weather data is trans-formed into Canadian Climate Centre format by Matlab®. The field data of leachate production, site plans, and design drawings are all obtained from the landfill operators and environmental protection bureaus of local governments. The landfills are divided

into zones according to different surface slope or drainage slope. In a landfill, profile is established for each zone and calculated in Visual HELP. A profile across the whole landfill is built for slope stability analysis. The result of lateral leachate drainage and leachate head will be analyzed for sensitivity of parameters and compared with field data. Then, the resulted leachate head will be applied to slope stability analysis by SLOPE/W.

3.2 Computer Programs

3.2.1 Visual HELP

The input of Visual HELP can be defined as three parts, the weather data, landfill profile, and material parameters. There are two ways to import weather data for Visual HELP, that is by generating synthetic weather data or inputting historic weather data. Visual HELP incorporates Weather Generator, which is developed by U.S Department of Agriculture (Richardson and Wright, 1984). There are two formats for inputting historic weather data. The first one of two types is Canadian Climate Centre format, which includes the data of precipitation, temperature, and solar radiation. The other one is National Oceanic and Atmospheric Administration format, which includes the data of precipitation, minimum temperature, and maximum temperature.

The weather data such as precipitation, temperature, and solar radiation are all transformed into Canadian Climate Centre format by Matlab®. Afterward, the transformed weather data will be input into Visual HELP.

The site parameters of landfill includes area, runoff area, initial surface water, and vegetation class for general settings and slope degree, slope length, surface slope, surface slope length, and thickness of each layer.

The landfill is divided into 5 layers in Visual HELP: vertical percolation layer,

lateral drainage layer, barrier soil liner, geomembrane liner, and geotextiles and geonets. Moreover, there are default materials to build the profile of landfill. Except for geomembrane layer, six material parameters can be edited for the other layers, including total porosity, wilting point, saturated hydraulic conductivity, subsurface inflow, and initial moisture content. For the material parameters of geomembrane layer, there are pinhole density, installation defects, placement quality, and geotextile transmissivity for editing.

The flow chart for Visual HELP analysis is shown in Figure 3-2.

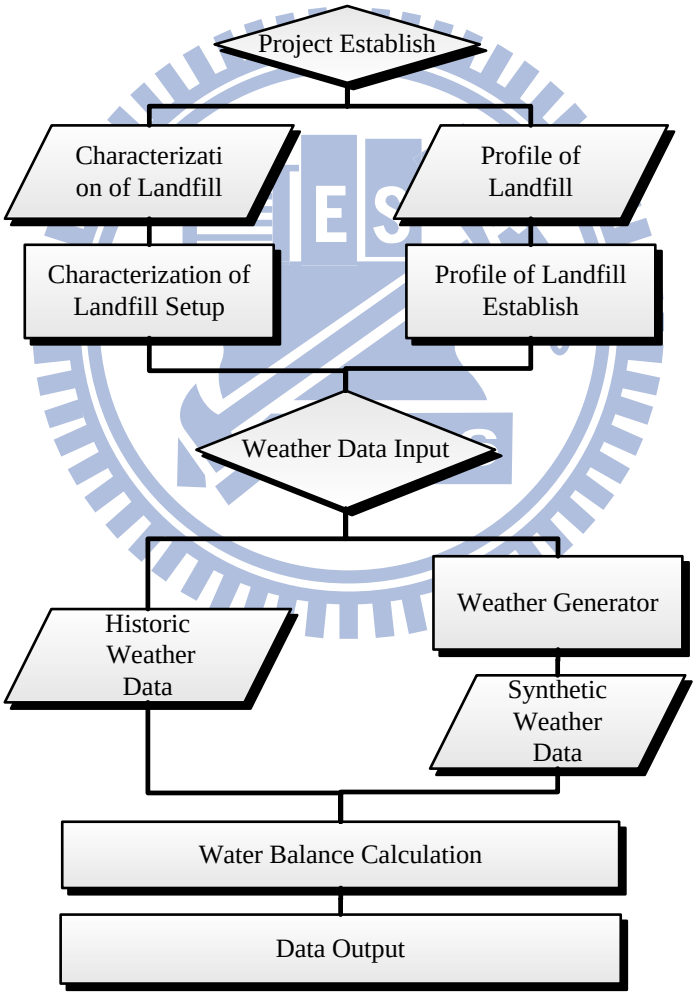

Figure 3-2: Flow Chart for Visual HELP Analysis

3.2.2 SLOPE/W

Site Establishment for Analysis

Site profile is built by graphical user interface. The build of profile includes the geometry of the site, pore water pressure, external stress, anchor force, reinforcement, ground acceleration. The pore water pressure can be imported as pore water pressure ratio, Ru, and B-bar coefficients, or drawn as piezometric line and discrete points.

The parameters for building the profile for slope stability analysis include unit weight, cohesion, and internal friction angle.

Methods of Slope Stability Analysis

In this study, the failure surface of landfill is below the landfill and is irregular. Hence the calculation procedure by Morgenstern and Price are used. The failure surface is specified in the barrier layer since many failures occurred in the liner system. The procedure of slope stability analysis is shown in the flow chart in Figure 3-3.

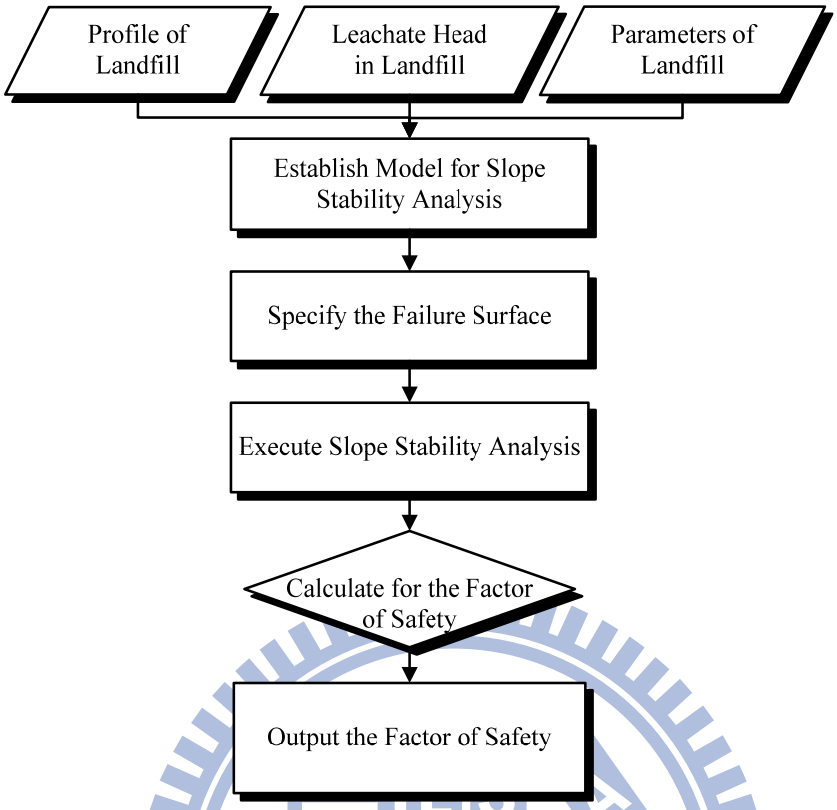

Figure 3-3: Flow Chart of Slope Stability Analysis

3.3 Case Background

Three landfills, Bali Landfill, Toufen Landfill, and Anding Landfill, are selected in this study. The main characteristic of these three landfills are list in Table 3-1. These landfills are chosen from the northern, middle, and southern of Taiwan. Meanwhile, the wastes in three landfills are all different from each other. Bali Landfill and Toufen Landfill are located in the valleys and hence the slope stability analysis will be applied on these two landfills. Anding Landfill is located in a plain so there is no necessary to apply slope stability analysis on this landfill.

Table 3-1: Main Characteristic of Selected Landfill

	Bali Landfill	**Toufen Landfill**	**Anding Landfill**
Location	North of Taiwan	Middle of Taiwan	South of Taiwan
Landform	Valley	Valley	Plain
Incoming Waste	MSW	MSW and Incinerator Fly Ash	Incinerator Fly Ash
Annual Precipitation (1989-2008)	2014 mm	1629 mm	1433 mm

3.3.1 Bali Landfill

Site Characteristic and Operation

Bali Landfill is located in a valley by the coast in northern Taiwan. The total area of Bali Landfill is 596,900 m^2, which includes 118,626 m^2 of area for the first 3 period of operation. The full site view is shown in Figure 3-4. The Bali Landfill has been in operation from 1997 till now. The operation of Bali landfill is divided into 4 periods, including 1st period, 2nd period, 3rd period, and post-3rd period. In the first 3 periods, only municipal solid waste was filled in the landfill and the incoming waste is 1,100 ton/day. The incinerator ash is only accepted by post-3rd period, and leachate drained from post-3rd period is separated for the other periods. Therefore, the post-3rd period is not included in this study.

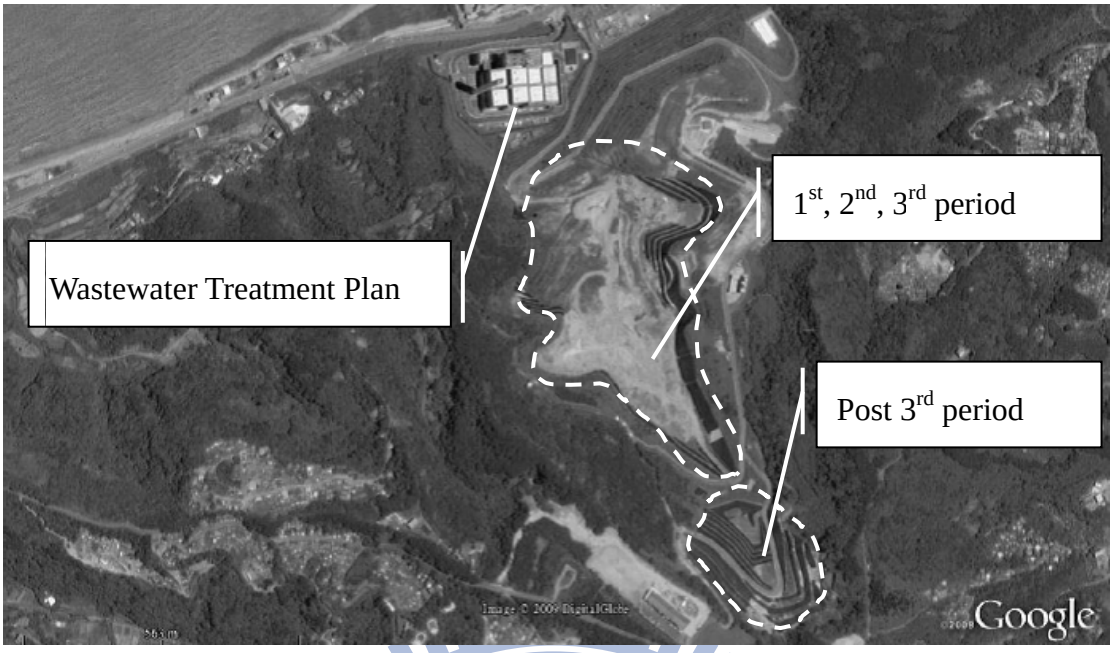

Figure 3-4: Geography of Bali Landfill, reprinted from Google Earth

Landfill Design

Bali Landfill is divided into 5 zones because of its irregular shape (Figure 3-5). Zone 1 has a very steep slope of bottom because this zone is facing the geotex-tile-reinforced wall. In comparison with the other 4 zones, the surface slope of zone 2 inclines rapidly. Zone 3 is disported due to the rapidly rising of the slope of bottom, and in contrast, the feature of Zone 4 is the relatively flat slope of bottom. Zone 5 is a V-shaped zone with flat surface. The central profile (Figure 3-6) for slope stability is based on the A-A' line in Figure 3-5.

According to the design data (Figure 3-7) provided from staff of Bali Landfill, the liner system only contains a drainage layer with 400 mm-diameter HDPE drainage pipes, loam fill, and a HDPE geomembrane layer for barrier. Figure 3-8 shows the profile for HELP. The height of waste layer, slope degree, and area differ from zone to zone.

The designed maximum quantity of daily leachate production treatment is 800

m^3 per day.

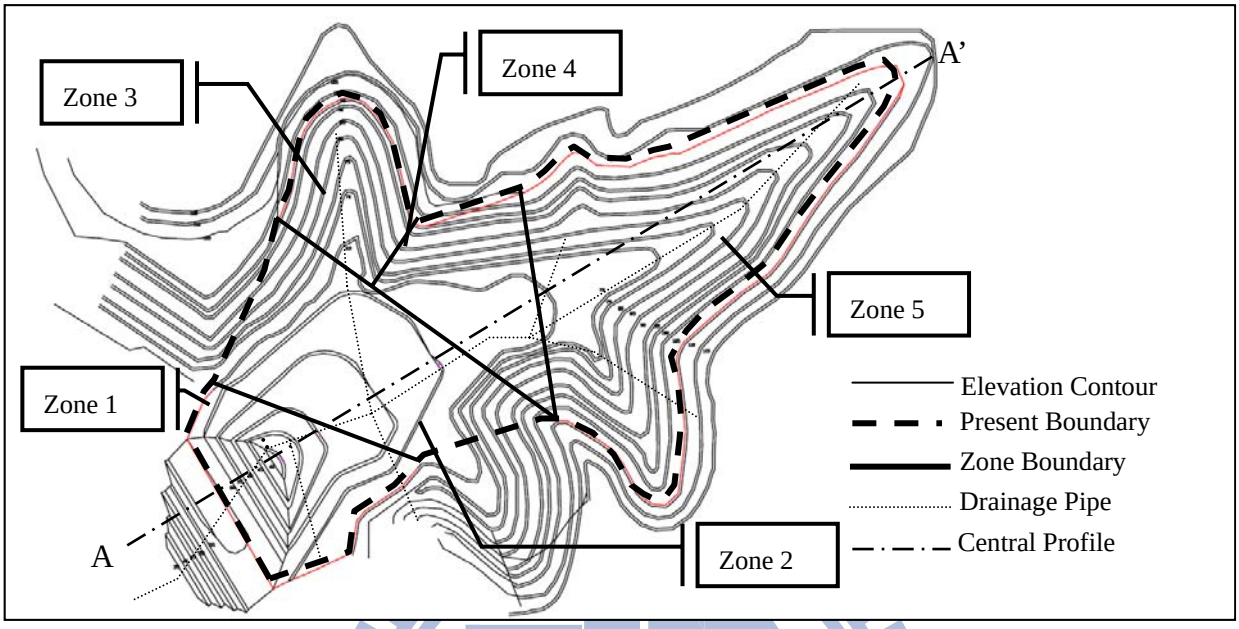

Figure 3-5: Bali Landfill from Plan View

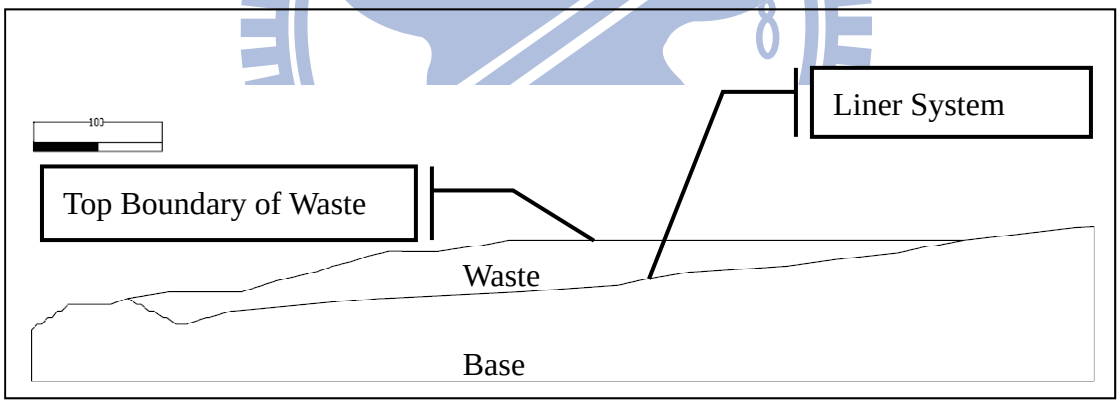

Figure 3-6: Profile of Bali Landfill for Slope Stability Analysis

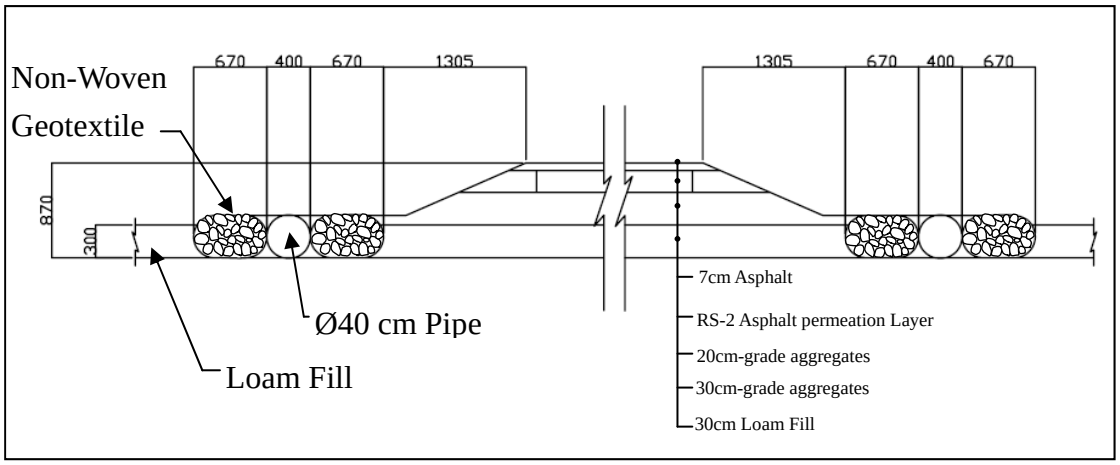

Figure 3-7: Design Profile of Main Road and Drainage Pipe, Redraw from the Original Drawing

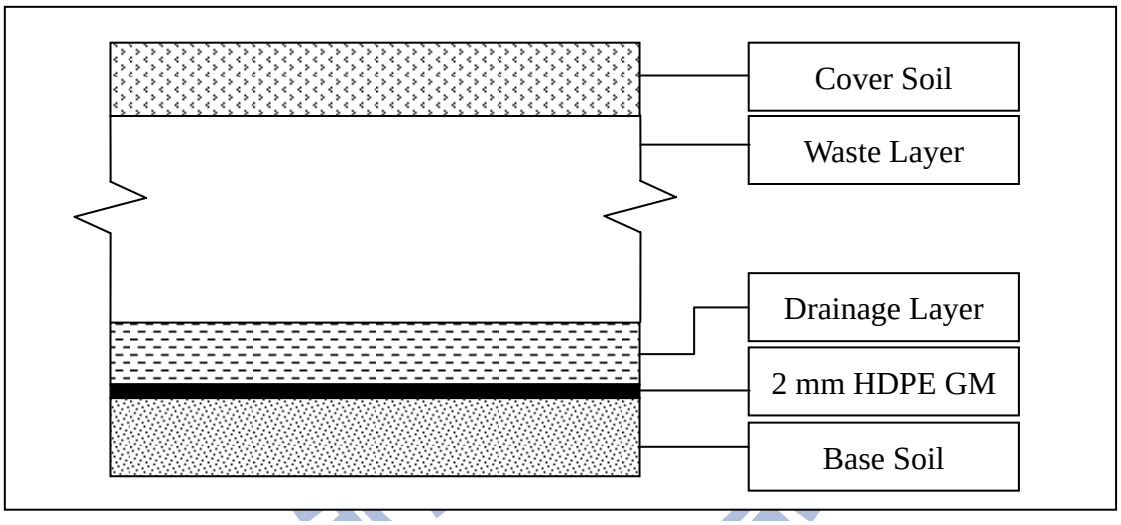

Figure 3-8: Profile of Bali Landfill for HELP

Climate

The weather data of Bali Landfill is obtained from Danshui Station. Considering the consistency of weather data, including daily precipitation, global solar radiation, daily temperature, quarterly relative humidity, and average wind speed, all weather data are selected from one weather station, No.466900 Danshui Station from 1989 to 2008.

The weather data of Bali Landfill is summarized in Table 3-2. The average annual precipitation is 2014 mm and the average annual mean temperature is 22.1°C. The average relative humidity is 79%. Therefore, the climate in Bali can be defined as

"humid climate".

Table 3-2: Summary of weather in Bali Landfill

	Maximum	Average	Minimum
Annual Precipitation	2865 mm	2014 mm	968 mm
Annual Mean Temperature	22.7 °C	22.1 °C	21.4 °C
Relative Humidity (quarterly)	89 %	79 %	74 %

3.3.2 Toufen Landfill

Site Characteristic and Operation

Toufen Landfill was located in a valley near Toufen Town, middle region of Taiwan. Toufen Landfill neighbors a closed landfill, (Figure 3-9). The total area of Toufen Landfill is 34,427 m^3, which includes 21,618 m^3 of the present fill area and 29,360 m^3 of closed fill area. The closed landfill is not included in this study. Toufen Landfill accepts municipal solid wastes, industrial wastes, and incinerator ash.

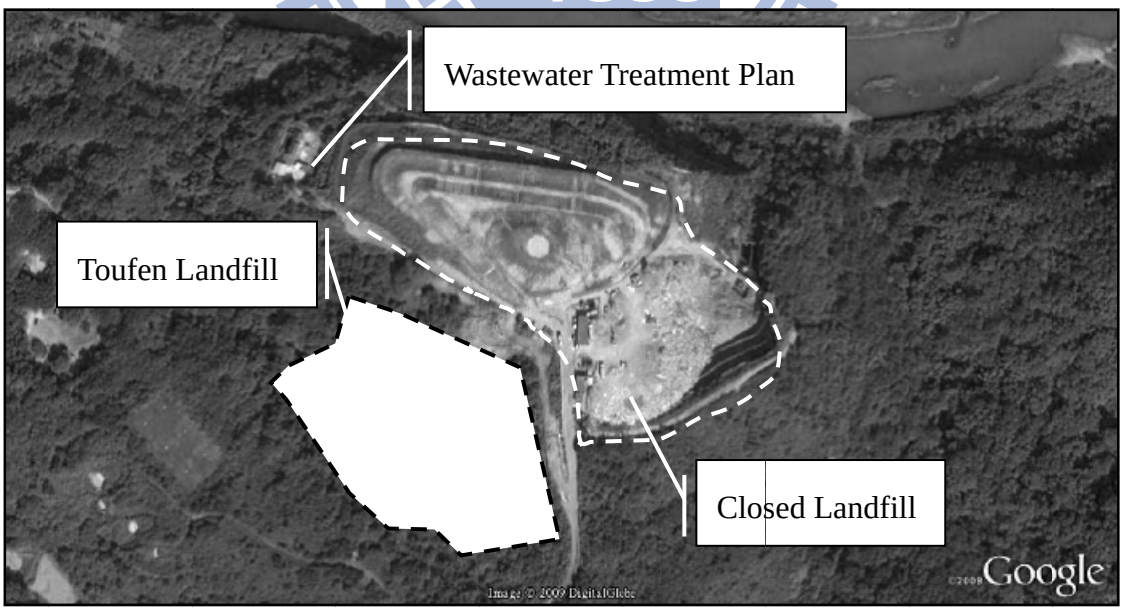

Figure 3-9: Geography of Toufen Landfill, reprinted from Google Earth

Landfill Operation and Design

Toufen Landfill is divided into 2 zones, which is shown in Figure 3-10. Zone 1 has a flat slope of bottom, and Zone 2 has a much steeper slope than Zone 1 because Zone 2 includes most slope area of Toufen Landfill. The central profile of Toufen Landfill is shown in Figure 3-11, which is based on the A-A' line in Figure 3-10.

The drainage layer is built with 600 mm-diameter HDPE pipes and loam fill. The barrier layer consists of a 2 mm thick HDPE geomembrane and a geosynthetic clay liner (GCL). The profile of Toufen Landfill is shown in Figure 3-12.

The designed maximum quantity of daily leachate production treatment is 250 m^3 per day.

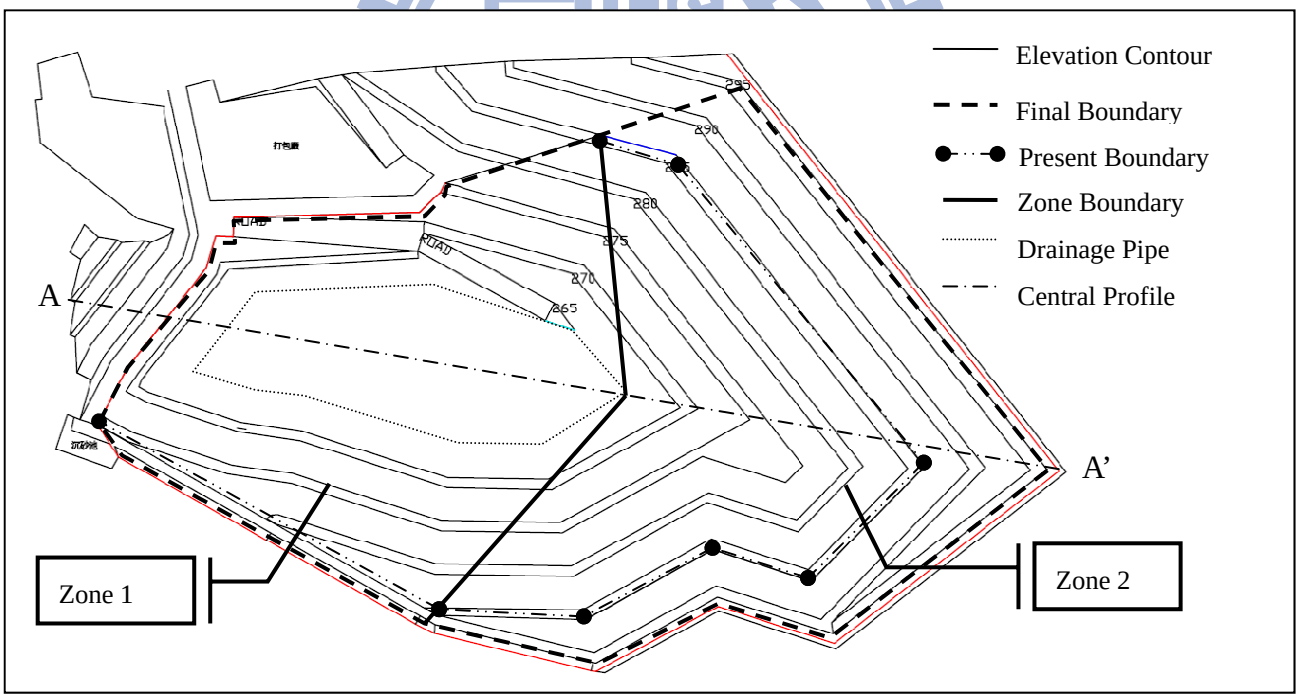

Figure 3-10: Toufen Landfill from Plan View, Redraw from the Origin Drawing

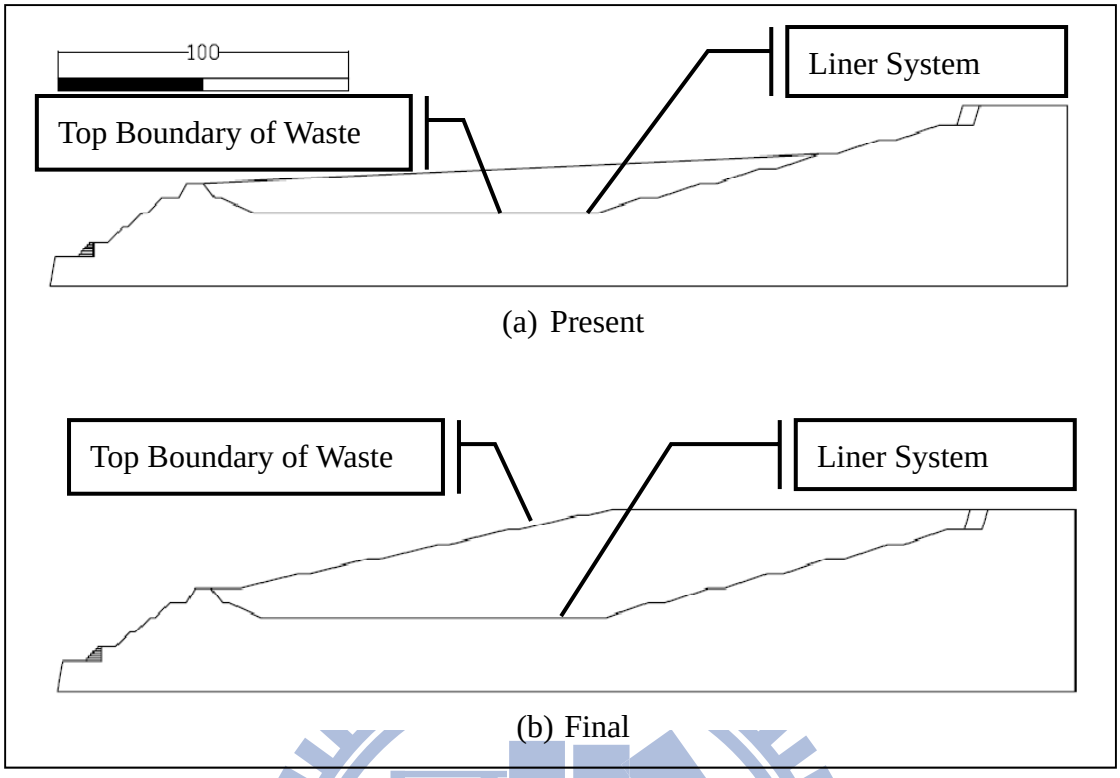

Figure 3-11: Profile of Toufen Landfill Side View

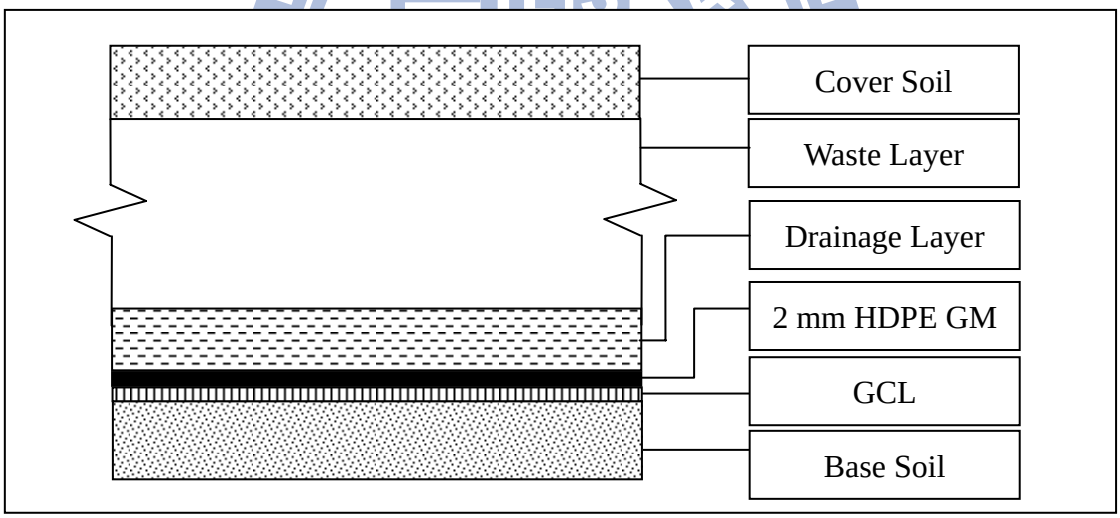

Figure 3-12: Profile of Toufen Landfill for HELP

Climate

The nearest weather station Jhunan Station is at a distance of 4.85 kilometers from Toufen Landfill and is capable to provide daily precipitation, daily temperature, and average wind speed. Because global radiation and relative humidity are available from few weather stations, these two data are obtained from Hsinchu Station, which is 21.28

kilometers away. The weather data were collected from 1993 to 2008.

The weather data of Toufen is summarized in Table 3-3. The average annual precipitation is 1629 mm and the average annual mean temperature is 22.3°C. The average relative humidity is 77%. Therefore, the climate of Toufen can be defined as “humid climate”.

Table 3-3: Summary of Weather in Toufen Landfill

	Maximum	Average	Minimum
Annual Precipitation	2192 mm	1629 mm	821 mm
Annual Mean Temperature	23.0 °C	22.3 °C	21.4 °C
Humidity (quarterly)	86 %	77 %	71 %

3.3.3 Tainan Anding Landfill

Site Characteristic and Operation

Tainan Anding Landfill is located in the middle of Tainan County, north of Tainan City. Anding Landfill is an above-ground-filled landfill, and the only source of waste is 180 ton/day incinerator ash from Yong-Kang Incinerator Plant. After being constructed in 2003, Anding Landfill has operated till now. Site view is shown in Figure 3-13. The present filled area of Anding Landfill is 27,086 m^2. The subsidiary wastewater treatment plant treats not only the leachate from Anding Landfill, but also the leachate from the landfills of neighboring towns.

Figure 3-13: Geography of Anding Landfill, reprinted from Google Earth

Landfill Design

According to the design drawing (Figure 3-14), Anding Landfill contains a double liner system. The primary liner system consists of a drainage layer filled with course sand and a barrier layer of 2 mm HDPE geomembrane. The secondary liner system consists of a drainage layer with HDPE drainage pipes and filled with course sand, and a barrier layer of 1.5 mm HDPE geomembrane. The profile of Anding Landfill is shown in Figure 3-16. Figure 3-17 indicates the whole profile which is based on the A-A' line in Figure 3-15. The top boundaries illustrate the geometry of present condition and the condition as reaching the level of designed fill limit. In addition, the designed fill limit is assumed to include two more levels for water balance analysis with the variation of height of waste increases to 25.1 m.

The slope of Anding landfill is uniform and the shape of landfill is similar to trapezium. Therefore, the landfill is analyzed as a whole without subdivided zones.

The designed maximum quantity of daily leachate production treatment is 600 m^3 per day.

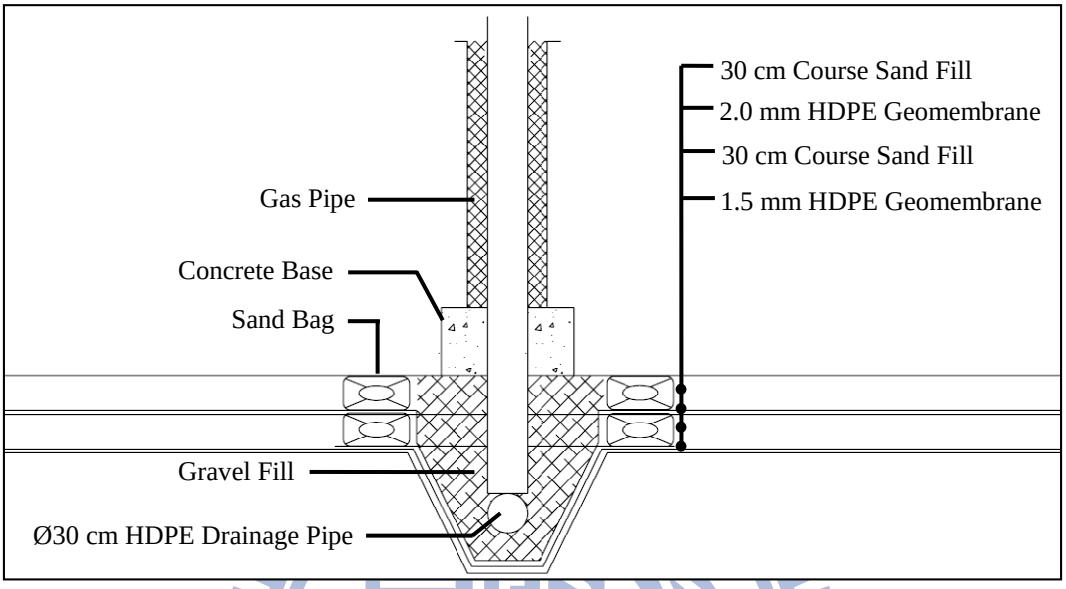

Figure 3-14: Detail of liner system of landfill

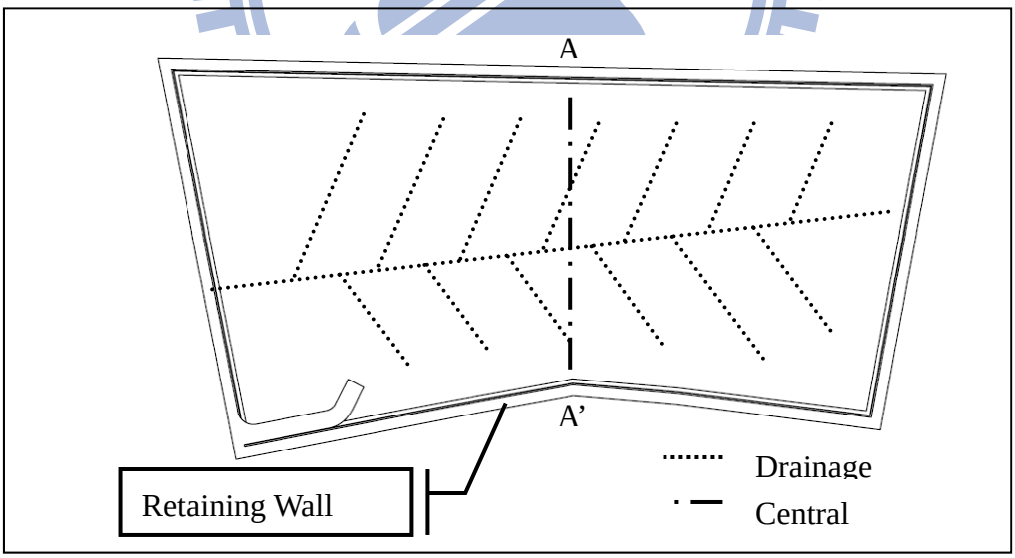

Figure 3-15: Anding Landfill from Plan View, Modified from the Original Drawing

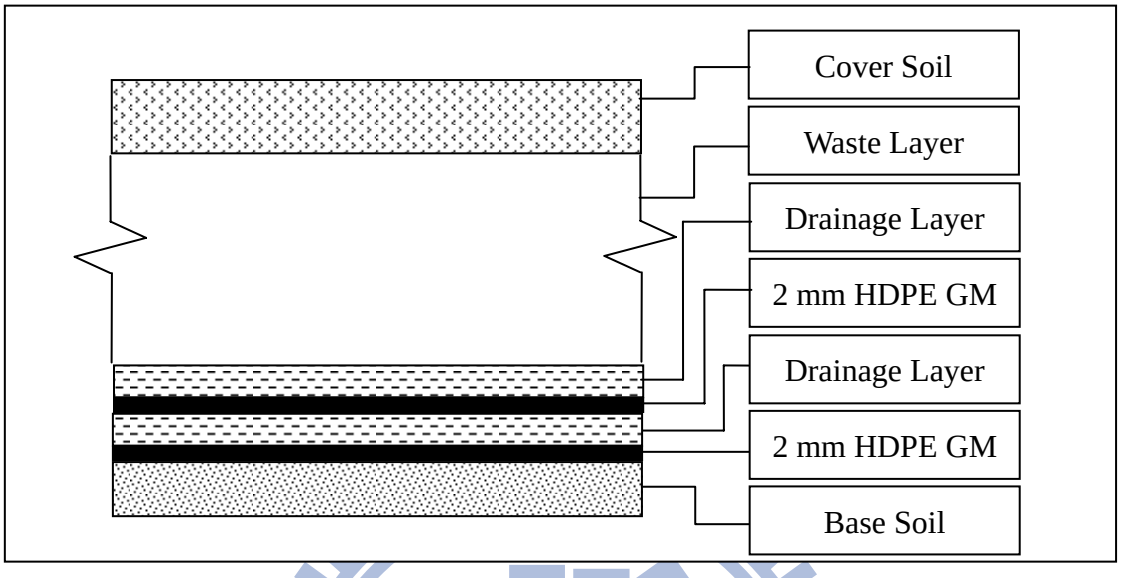

Figure 3-16: Profile of Anding Landfill for HELP

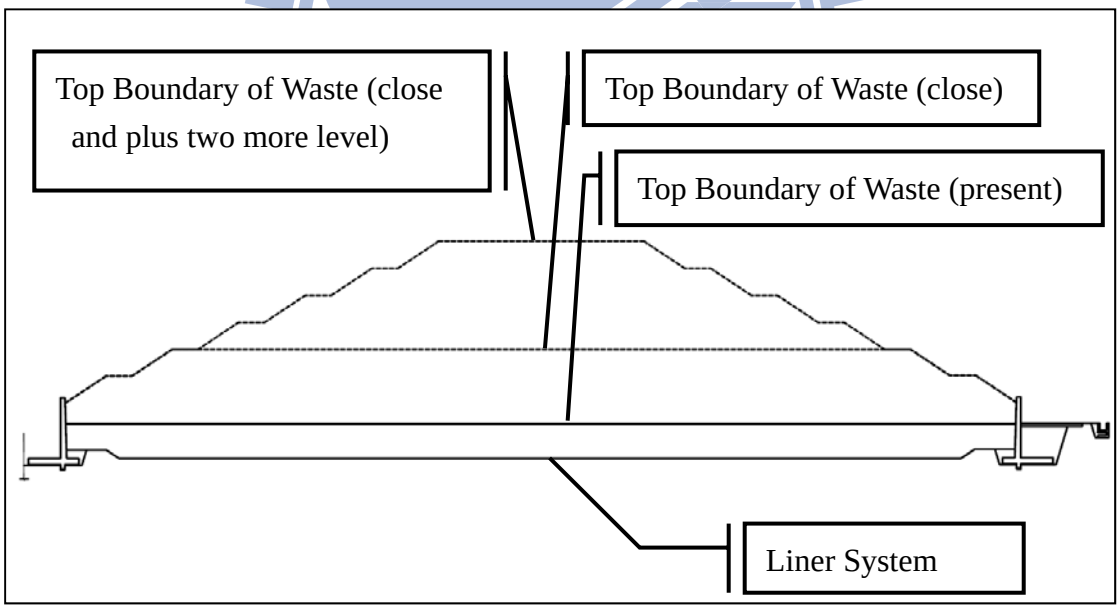

Figure 3-17: Profile of Anding Landfill Side View

Climate

The weather data is obtained from Tainan Station, which is 9.25 kilometers away from Anding Landfill. During 1998 to 2002, Tainan Station had been terminated and

the meteorological observation had been changed to Yong-Kang Station which is 3.73 kilometers away from Anding Landfill. Hence the weather data is not entirely consistent due to the move of weather station.

The weather data of Anding is summarized in Table 3-4. The average annual precipitation is 1433 mm and the average annual mean temperature is 24.4°C. The average relative humidity is 76%. Therefore, the climate of Toufen can be defined as “humid climate”.

Table 3-4: Summary of Climate in Anding

	Maximum	Average	Minimum
Annual Precipitation	2324 mm	1433 mm	428 mm
Annual Mean Temperature	25.1 °C	24.4 °C	23.6 °C
Humidity (quarterly)	85 %	76 %	70 %

3.4 Study Scheme for Sensitivity Analysis

The sensitivity analysis is categorized into 8 cases as shown in Table 3-5. For CASE 1, CASE 2, CASE 3, CASE 4, and CASE 5, the evaporative depth, the slope of LCRS, the hydraulic conductivity of LCRS, the hydraulic conductivity of waste, and the height of waste is varied, respectively. Moreover, as the waste reaches the design fill limit, CASE 6 is varied for the slope of LCRS; CASE 7 and CASE 9 is varied for the hydraulic conductivity of LCRS. In this table, the background in the cells of variation is filled with grey.

CASE 1-1 is defined as the initial case. In this case, hydraulic conductivities of waste and LCRS are representative of the most suitable condition of landfills in Taiwan. Furthermore, CASE 1-1 also equals to CASE 3-1, CASE 4-1, and CASE 5-1 because the parameters in CASE 1-1 are the initial value of evaporative depth, hydraulic conductivity of LCRS and waste, and height of the waste. Hence the series of CASE 3, CASE 4, and CASE 5 starts with CASE 1-1.

In the series of CASE 3, the average slope of LCRS will be applied in HELP. Anding Landfill is not included in this case due to its homogeneous slope (0.5%). From CASE 3-2 to CASE 3-8, the variation is the hydraulic conductivity of LCRS. The hydraulic conductivity of LCRS will be applied from K_{max} to 1×10^{-7} cm/s. From CASE 4-2 to CASE 4-5, the variation is the hydraulic conductivity of waste. From Case 5-1 to CASE 5-3, the variation is the height of the waste. This series of case is only applied for Toufen Landfill and Anding Landfill.

The series of CASE 6 and CASE 7 are all calculated as the waste layer reach the designed fill limit. In addition, the series of CASE 9 is calculated as the waste layer plus two more layer of waste. From CASE 6-2 to CASE 6-8, the variation is the slope of LCRS. The variation in series of CASE 7 and CASE 9 is the hydraulic conductivity

of LCRS. Bali Landfill is close to the design fill limit, thus the variation of height of waste will not apply in the simulation of Bali Landfill.

Table 3-5: Values of Cases for Sensitivity Analysis

Case No.	Evaporative Depth (cm)	Slope of LCRS (%)		Hydraulic conductivity of LCRS (cm/s)	Hydraulic conduc-tivity of Waste (cm/s)		Height of Waste (m)		
	B[*1],T[*2],A[*3]	B	T	B,T,A	B,T	A	B	T	A
CASE 1-1	3	Various[*4]		K_{max}[*5]	1×10^{-3}	1×10^{-2}	P[*7]	P	P
CASE 1-2	15	Various		K_{max}	1×10^{-3}	1×10^{-2}	P	P	P
CASE 1-3	30	Various		K_{max}	1×10^{-3}	1×10^{-2}	P	P	P
CASE 2-1	3	0	0	K_{max}	1×10^{-3}	1×10^{-2}	P	P	X[*6]
CASE 2-2	3	1	1	K_{max}	1×10^{-3}	1×10^{-2}	P	P	X
CASE 2-3	3	2	3	K_{max}	1×10^{-3}	1×10^{-2}	P	P	X
CASE 2-4	3	3	5	K_{max}	1×10^{-3}	1×10^{-2}	P	P	X
CASE 2-5	3	4	7	K_{max}	1×10^{-3}	1×10^{-2}	P	P	X
CASE 2-6	3	5	9	K_{max}	1×10^{-3}	1×10^{-2}	P	P	X
CASE 2-7	3	6	9.45	K_{max}	1×10^{-3}	1×10^{-2}	P	P	X
CASE 2-8	3	6.76	11	K_{max}	1×10^{-3}	1×10^{-2}	P	P	X
CASE 2-9	3	7		K_{max}	1×10^{-3}	1×10^{-2}	P	P	X
CASE 3-2	3	Various		1×10^{-1}	1×10^{-3}	1×10^{-2}	P	P	P
CASE 3-3	3	Various		1×10^{-2}	1×10^{-3}	1×10^{-2}	P	P	P
CASE 3-4	3	Various		1×10^{-3}	1×10^{-3}	1×10^{-2}	P	P	P
CASE 3-2	3	Various		1×10^{-1}	1×10^{-3}	1×10^{-2}	P	P	P
CASE 3-3	3	Various		1×10^{-2}	1×10^{-3}	1×10^{-2}	P	P	P
CASE 3-4	3	Various		1×10^{-3}	1×10^{-3}	1×10^{-2}	P	P	P
CASE 3-5	3	Various		1×10^{-4}	1×10^{-3}	1×10^{-2}	P	P	P
CASE 3-6	3	Various		1×10^{-5}	1×10^{-3}	1×10^{-2}	P	P	P
CASE 3-7	3	Various		1×10^{-6}	1×10^{-3}	1×10^{-2}	P	P	P
CASE 3-8	3	Various		1×10^{-7}	1×10^{-3}	1×10^{-2}	P	P	P
CASE 4-2	3	Various		K_{max}	1×10^{-4}	1×10^{-3}	P	P	P
CASE 4-3	3	Various		K_{max}	1×10^{-5}	1×10^{-4}	P	P	P
CASE 4-4	3	Various		K_{max}	X	1×10^{-5}	X	X	P

Table 3-5: Values of Cases for Sensitivity Analysis (Continued)

Case No.	Evaporative Depth (cm)	Slope of LCRS (%)		Hydraulic conductivity of LCRS (cm/s)	Hydraulic conduc-tivity of Waste (cm/s)		Height of Waste (m)		
	B[*1],T[*2],A[*3]	B	T	B,T,A	B,T	A	B	T	A
CASE 5-2	3	Various		K_{max}	1×10^{-3}	1×10^{-2}	X	X	C[*8]
CASE 5-3	3	Various		K_{max}	1×10^{-3}	1×10^{-2}	X	X	C+2[*9]
CASE 6-1	3	X	0	K_{max}	1×10^{-3}	1×10^{-2}	X	C	X
CASE 6-2	3	X	1	K_{max}	1×10^{-3}	1×10^{-2}	X	C	X
CASE 6-3	3	X	3	K_{max}	1×10^{-3}	1×10^{-2}	X	C	X
CASE 6-4	3	X	5	K_{max}	1×10^{-3}	1×10^{-2}	X	C	X
CASE 6-5	3	X	7	K_{max}	1×10^{-3}	1×10^{-2}	X	C	X
CASE 6-6	3	X	9	K_{max}	1×10^{-3}	1×10^{-2}	X	C	X
CASE 6-7	3	X	9.45	K_{max}	1×10^{-3}	1×10^{-2}	X	C	X
CASE 6-8	3	X	11	K_{max}	1×10^{-3}	1×10^{-2}	X	C	X
CASE 7-2	3	Various		1×10^{-1}	1×10^{-3}	1×10^{-2}	X	C	C
CASE 7-3	3	Various		1×10^{-2}	1×10^{-3}	1×10^{-2}	X	C	C
CASE 7-4	3	Various		1×10^{-3}	1×10^{-3}	1×10^{-2}	X	C	C
CASE 7-5	3	Various		1×10^{-4}	1×10^{-3}	1×10^{-2}	X	C	C
CASE 7-6	3	Various		1×10^{-5}	1×10^{-3}	1×10^{-2}	X	C	C
CASE 7-7	3	Various		1×10^{-6}	1×10^{-3}	1×10^{-2}	X	C	C
CASE 7-8	3	Various		1×10^{-7}	1×10^{-3}	1×10^{-2}	X	C	C
CASE 9-2	3	Various		1×10^{-1}	X	1×10^{-2}	X	X	C+2
CASE 9-3	3	Various		1×10^{-2}	X	1×10^{-2}	X	X	C+2
CASE 9-4	3	Various		1×10^{-3}	X	1×10^{-2}	X	X	C+2
CASE 9-5	3	Various		1×10^{-4}	X	1×10^{-2}	X	X	C+2
CASE 9-6	3	Various		1×10^{-5}	X	1×10^{-2}	X	X	C+2
CASE 9-7	3	Various		1×10^{-6}	X	1×10^{-2}	X	X	C+2
CASE 9-8	3	Various		1×10^{-7}	X	1×10^{-2}	X	X	C+2

*1: B = Bali Landfill

*2: T = Toufen Landfill

*3: A = Anding Landfill

*4: Various: slope of LCRS is different from zone to zone

*5: K_{max} = max hydraulic conductivity of LCRS

*6: X = Not included in this case

*7: P = Present Height;

*8: C = Closed (Reach designed fill limit)

*9: C+2 = Closed with 2 more levels

The result of daily and cumulative leachate production will be compared to the field data. The difference between simulation and field data will be quantified by root mean square method. The difference will be calculated from the first date of the field data.

Since there is no research on hydraulic conductivity of waste in landfills in Taiwan, the hydraulic conductivity has to be adopted from foreign researches of landfills (Table 2-4). The hydraulic conductivity of waste layer is assumed to be 1×10^{-3} cm/s for MSW and 1×10^{-2} cm/s for incinerator fly ash. In order to obtain conservative results, the evaporative depth is set to be 3 cm in the initial condition for ensuring the maximum leachate collection.

Derivation of K_{max}

The total quantity of leachate is Q and the hydraulic conductivity of drainage layer is K_{max}. As shown in Figure 3-18, the drainage layer consists of the drainage pipe and the loam material such as MSW hence the total quantity of leachate collection from drainage layer is also consisted from drainage pipe, Q_{pipe}, and loam material, Q_{loam}. Since:

$$Q_{max} = Q_{pipe} + Q_{loam}, \quad \text{.....(3.1)}$$

$$Kmax \cdot i \cdot A_{total} = K_{pipe} \cdot i \cdot A_{pipe} + K_{loam} \cdot i \cdot A_{loam}, \quad \text{.....(3.2)}$$

where K_{pipe}=hydraulic conductivity of drainage pipe, which is assumed as 1 m/sec; A_{pipe}=area of drainage pipe; K_{loam}=hydraulic conductivity of loam material of the drainage layer, such as MSW (K = 0.001 cm/s); A_{loam}=area of loam material of the drainage layer. A_{total}=Total area of the drainage layer, which is: $A_{total} = A_{pipe} + A_{loam}$.

The hydraulic gradient, *i*, is constant in drainage layer and it is also the same value in the drainage pipe and loam material. Therefore, both *i* are all removed from the

equation and the equation shows:

$$K_{max} = \frac{K_{pipe}A_{pipe}}{A_{Total}} + \frac{K_{loam}A_{loam}}{A_{Total}} \quad \text{.....(3.3)}$$

The calculation result of K_{max} for Bali Landfill, Toufen Landfill, and Anding Landfill are listed in Table 3-6.

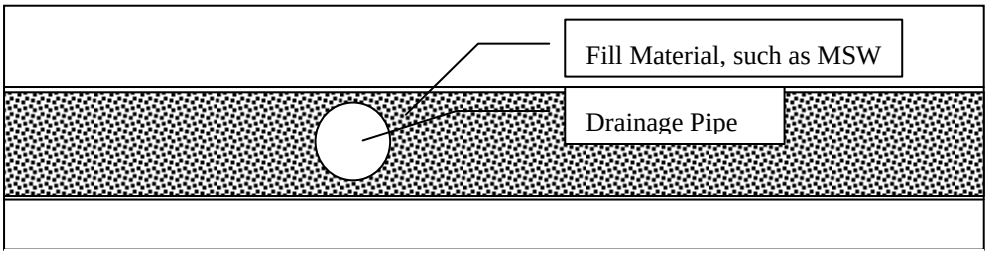

Figure 3-18: Profile of Drainage Layer

Table 3-6: Result of K_{max}

Name	**Bali Landfill**	**Toufen Landfill**	**Anding Landfill**
Width of Area	144 m	169 m	137 m
Diameter of Drainage Pipe	400 mm	600 mm	300 mm
K_{max} (cm/s)	0.175	0.3345	0.679

To get conservative result, the runoff is assumed as zero and the vegetation class is set as bare soil. Above two parameters of HELP is in order to produce the maximum amount of leachate.

Slope Stability Analysis

The profile of landfill is divided into three layers, waste layer, barrier layer, and the base layer. The base material of the landfill is assumed as soft rock. The unit weight of the soft rock is 24 kN/m^3. According to the strength of classification from ISRM (ISRM, 1981), the uniaxial compressive strength of the extremely weak rock is 250 kPa to 1000 kPa. In this study, the undrained cohesion is 250 kPa for obtaining conserva-

tional result. The stability analysis only calculates the factor of safety for the translational failure, thus the material strength of base soil does not affect the result of analysis.

The assumption of unit weight and shear strength are based on the result of field study in Taiwan (Fan and Shan, 2007). The material properties of waste are 10 kN/m^3 for unit weight, 35° for friction angle, and 34 kPa for cohesion which are conducted from in-situ direct shear tests in Jhunan Landfill and Hukou Landfill.

Based on the research on interface strength of geosythetics, the interfacial shear strength between HDPE and soil is assumed as 15° for friction angle (Liu, 2004) and 0 kPa for cohesion. In additional, the internal friction angle is assumed as 8° for the condition of wetting under the geomembrane. Though geomembrane is only 2 mm, the ground surface is not completely flat in the landfill. Therefore, the thickness of liner system is set as 0.1 m.

The parameters for slope stability analysis are summarized in Table 3-7

Table 3-7: Summary of Parameters for Slope Stability Analysis

	Waste Layer	**Barrier Layer**	**Base Layer**
Unit Weight (kN/m^3)	10	10	24
Cohesion (kPa)	34	0	250 (S_u)
Friction Angle (°)	35	15	

Su = Undrained Shear Strength

Chapter 4 Result and Discussion

4.1 Water Balance Analysis

4.1.1 Bali Landfill

The summary of Visual HELP analysis for Bali Landfill is listed in Table 4-1.

Table 4-1: Summary of Simulation Result of Bali Landfill from HELP

	Case 1-1	Case 1-2	Case 1-3	Case 2-1	Case 2-2	Case 2-3	Case 2-4	Case 2-5
Difference*(m^3)	357.7	359.6	393.5	283.5	294.0	313.2	328.0	338.0
CLP* (m^3)	459,790	327,741	260,033	441,192	450,774	455,279	457,172	458,140
MDL* (m^3)	1,360	1,069	752	1,039	1,162	1,172	1,265	1,308
H1* (m)	0.017	0.013	0.009	0.516	0.263	0.142	0.103	0.080
H2 (m)	0.026	0.020	0.015	0.508	0.254	0.129	0.090	0.071
H3 (m)	0.012	0.009	0.006	0.336	0.173	0.102	0.070	0.053
H4 (m)	0.075	0.053	0.040	0.601	0.276	0.144	0.103	0.081
H5 (m)	0.023	0.018	0.013	0.406	0.222	0.113	0.080	0.062
	Case 2-6	**Case 2-7**	**Case 2-8**	**Case 2-9**	**Case 3-1**	**Case 3-2**	**Case 3-3**	**Case 3-4**
Difference (m^3)	345.0	350.0	352.7	353.7	357.7	346.4	285.8	310.9
CLP (m^3)	458,717	459,098	459,295	459,367	459,790	458,880	444,127	394,402
MDL (m^3)	1,331	1,343	1,349	1,351	1,360	1,330	1,067	1,062
H1 (m)	0.065	0.054	0.049	0.047	0.017	0.028	0.267	2.239
H2 (m)	0.059	0.050	0.045	0.043	0.026	0.045	0.353	2.628
H3 (m)	0.043	0.036	0.033	0.031	0.012	0.020	0.162	2.122
H4 (m)	0.067	0.057	0.052	0.049	0.075	0.118	2.408	4.350
H5 (m)	0.050	0.042	0.038	0.036	0.023	0.041	0.326	2.422
	Case 3-5	**Case 3-6**	**Case 3-7**	**Case 3-8**	**Case 4-1**	**Case 4-2**	**Case 4-3**	
Difference (m^3)	356.0	360.0	357.4	356.6	357.7	354.3	449.8	
CLP (m^3)	381,453	379,970	379,339	379,385	459,790	439,531	294,923	
MDL (m^3)	1,297	1,243	1,281	1,281	1,360	1,316	980	
H1 (m)	2.309	2.322	2.329	2.323	0.017	0.017	0.011	
H2 (m)	2.676	2.682	2.692	2.692	0.026	0.025	0.020	
H3 (m)	2.243	2.244	2.234	2.235	0.012	0.012	0.008	
H4 (m)	4.407	4.420	4.423	4.423	0.075	0.068	0.055	
H5 (m)	4.056	4.066	4.065	4.066	0.023	0.023	0.017	

Difference: Calculated by root mean square method; CLP: Cumulative Leachate Production;
MDL: Maximum Daily Leachate; H1: Highest Leachate Head in Zone 1, similar to H2, H3, etc.

Figure 4-1 shows the cumulative leachate production of the most suitable condition and the field data. The cumulative leachate production from field data is 550,618 m^3 and the cumulative leachate production of CASE 1-1 is 459,789 m^3, which is the maximum among the cases and the closest to the field data. The difference is calculated by root mean square method and the smallest one is 283.5 m^3 which is obtained from CASE 2-1. It shows that the simulation of leachate production approaches the field data when the slope of LCRS is 0 %. Though the difference of CASE 2-1 is relative small to the other cases, the leachate production is only 441,191 m^3. Therefore, the difference is less in CASE 2-1 but the accumulative leachate production in CASE 1-1 is closer to the field data.

The variation of leachate production with the evaporative depth is shown in Figure 4-2. It indicates that while the evaporative depth increases from 3 cm to 30 cm, the cumulative decreases from 459,790 m^3 to 260,033 m^3. The maximum daily leachate production decreases from 1,360 m^3 to 752 m^3 due to the increase of the evaporation. The daily leachate production is shown in Figure 4-3. Figure 4-4 provides a close observation of daily leachate production between 2007/6/1 and 2007/9/1. It can be seen that though the evaporation increases, the time lag of leachate increases only within 4 days. The time lag of leachate production is similar with different evaporative depth hence the evaporation mainly affects the leachate production.

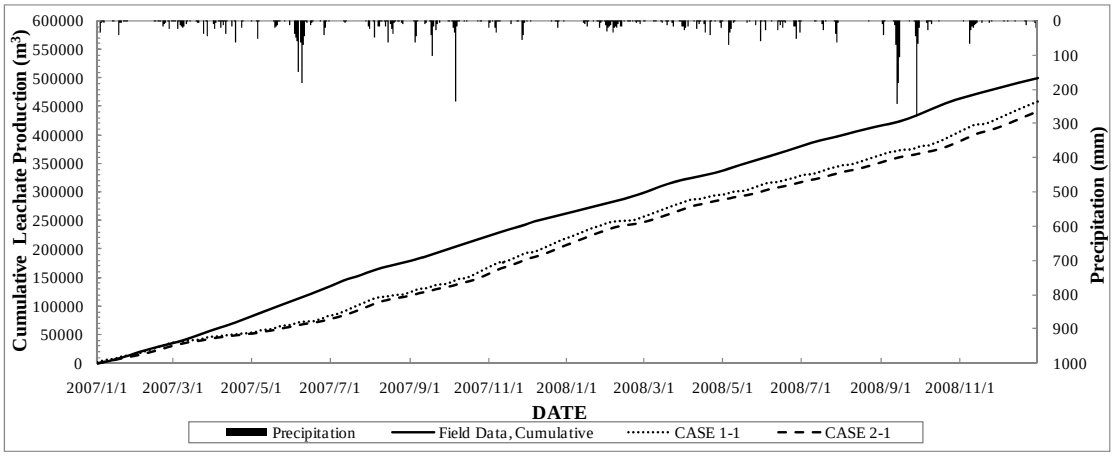

Figure 4-1: Cumulative Leachate Collection

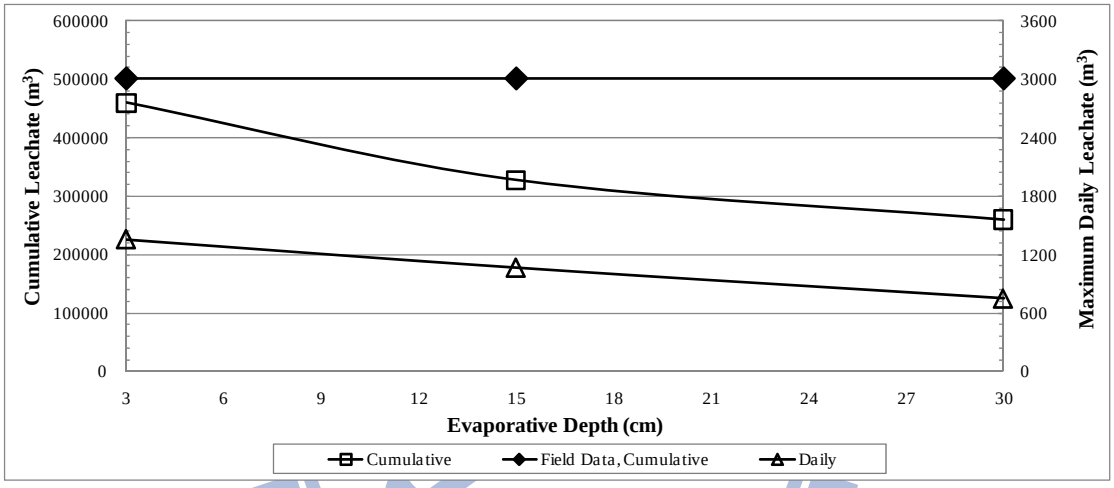

Figure 4-2: Variation of Leachate Production with Evaporative Depth

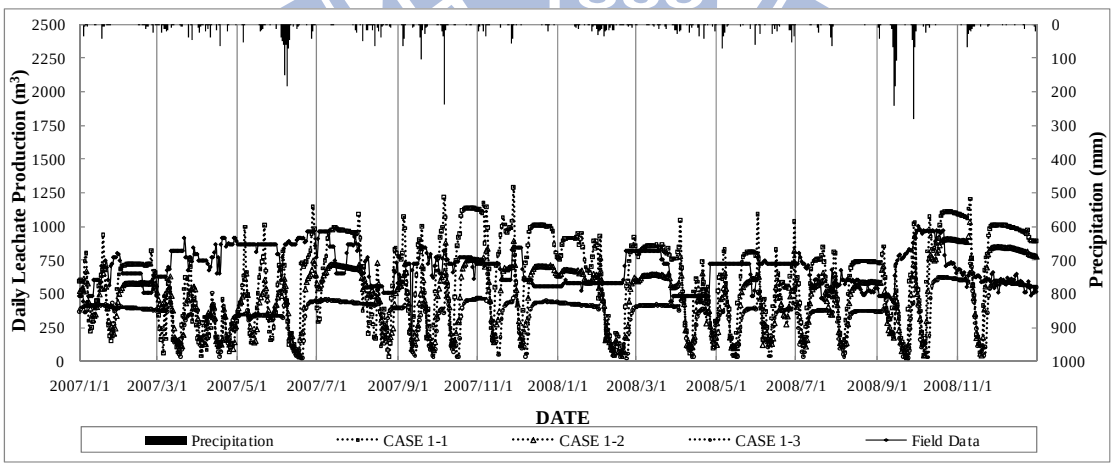

Figure 4-3: Variation of Daily Leachate Production with Evaporative Depth

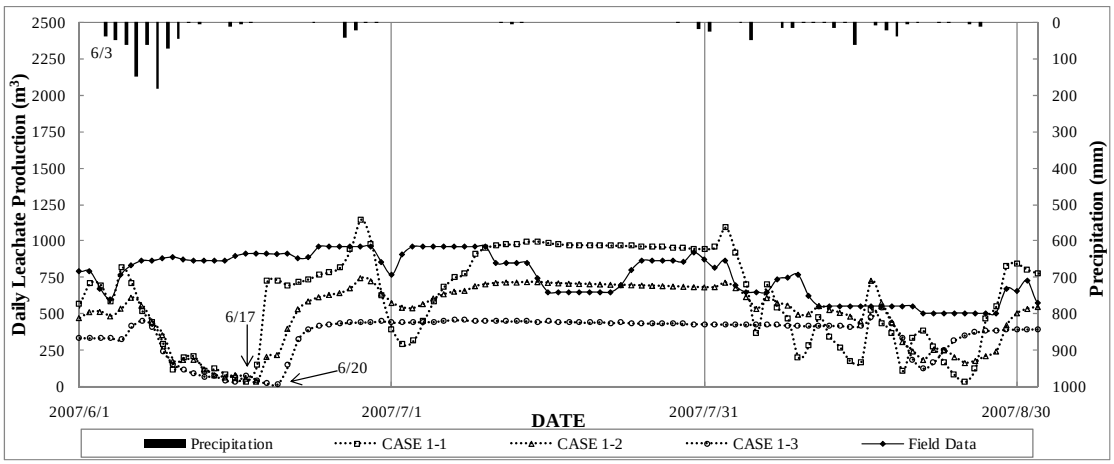

Figure 4-4: Variation of Daily Leachate Production with Evaporative Depth, between 2007/6/1 and 2007/9/1

Figure 4-5 shows the result variation of leachate production with the slope of LCRS. Figure 4-6 shows the result of highest leachate head in each zone of Bali Landfill with the change of slope. The increase of leachate production and decrease of highest leachate head are due to the increase of slope of LCRS. The cumulative leachate production increases from 441,191 m^3 to 459,367 m^3 while the slope increases to 7%. In addition, the daily leachate production increases from 1,038 m^3 to 1,349 m^3 while the cumulative leachate production tends to be stable after slope is steeper than 4%. In each zone of Bali Landfill, the highest leachate head also tends to reach stable.

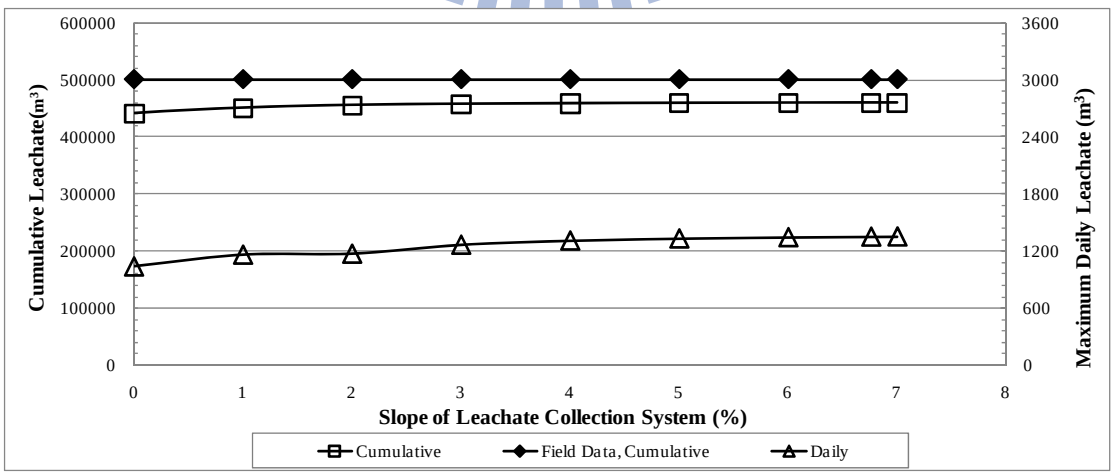

Figure 4-5: Variation of Leachate Production with LCRS Slope

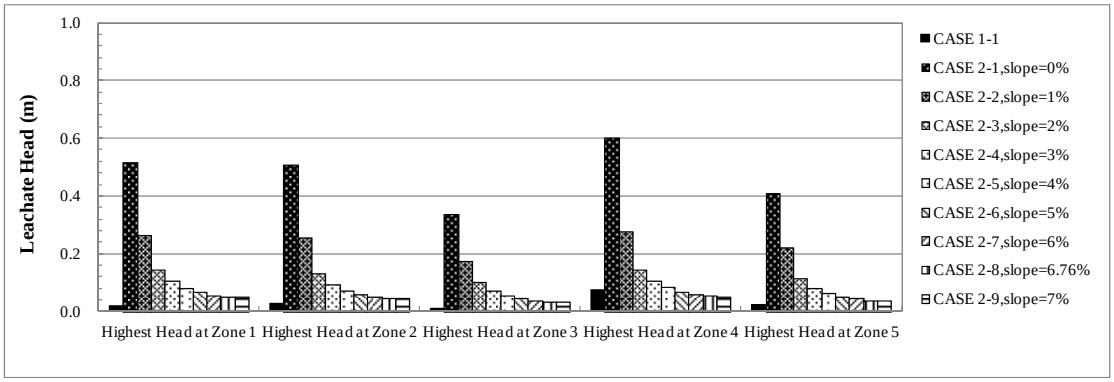

Figure 4-6: Variation of Leachate Head with LCRS Slope

Figure 4-7 shows the variation of leachate production and highest leachate head with the hydraulic conductivity of LCRS. The cumulative leachate production reduces from 459,790 m^3 to 379,385 m^3 when the hydraulic conductivity of LCRS decreases from 0.175 cm/s to 1.0×10^{-4} cm/s. The reduction of leachate production approaches to about 379,000 m^3 due to the calculation method of HELP. In HELP, the leachate production is governed by lateral drainage. Once the leachate head is higher than drainage layer, the drainage rate will include the layer above lateral drainage layer into calculation. In this study, the layer above LCRS is the waste layer. The hydraulic conductivity of waste layer is larger than the LCRS for more than 1 to 3 orders of magnitude when the hydraulic conductivity of LCRS is lower than 0.001 cm/s. Therefore, the flow rate is controlled by the hydraulic conductivity of waste layer when the leachate head is higher than LCRS.

Figure 4-8 shows the relation between leachate production and the hydraulic conductivity of waste. While the hydraulic conductivity of waste decreases by 2 orders of magnitude, the cumulative leachate production reduces from 459,790 m^3 to 294,923 m^3. The daily leachate production reduces from 1,360 m^3 to 980 m^3. The increase of hydraulic conductivity of waste causes the leachate head to rise. The evaporation does not increase with the decrease of flow rate hence there is no reduction for

the leachate produced by precipitation. Therefore, the increase of hydraulic conductivity of waste causes the leachate head to rise.

As shown in Figure 4-9, the decrease of hydraulic conductivity of waste causes the increase of time lag of leachate production. In Figure 4-9, the hydraulic conductivities of waste for CASE 1-1, CASE 4-2, CASE 4-3 are 1×10^{-3} cm/s, 1×10^{-4} cm/s, 1×10^{-5} cm/s, respectively. There is one rainfall started at 6/3. After 11 days, the decreasing leachate production begins to increase in CASE 1-1. With the decrease of hydraulic conductivity of waste, the time lag increases to 17 days in CASE 4-2 and over 1 month in CASE 4-3. Moreover, the amount of leachate and the leachate production rate is different among CASE 1-1 to CASE 4-3. In CASE 1-1, the leachate production increases rapidly with the precipitation. In CASE 4-3, the leachate production is lag to increase and amplitude of increase is not as high as CASE 1-1. It shows that the leachate production is less sensitive to the precipitation when the leachate production rate is lower. In addition, while the hydraulic conductivity of waste is lower, the time lag of leachate production is longer.

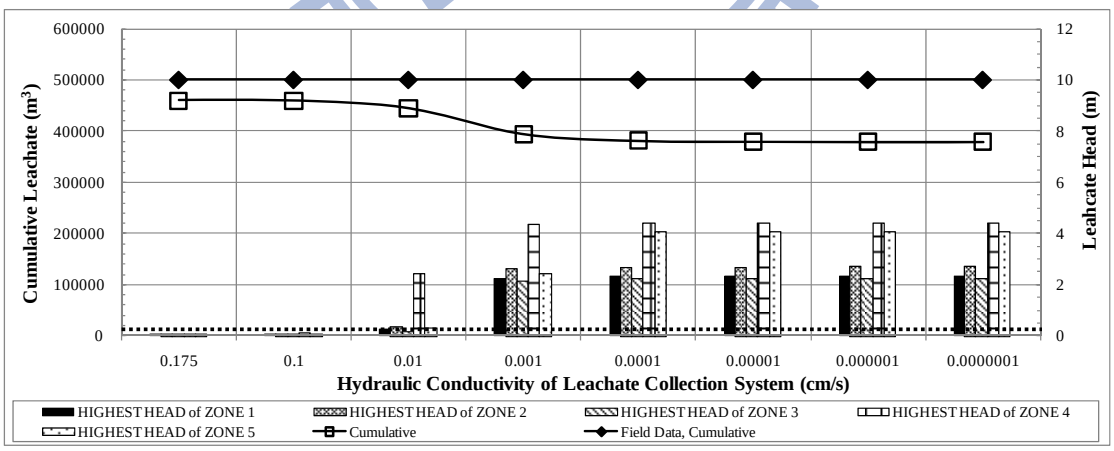

Figure 4-7: Variation of Leachate Production and Leachate Head with hydraulic Conductivity of LCRS

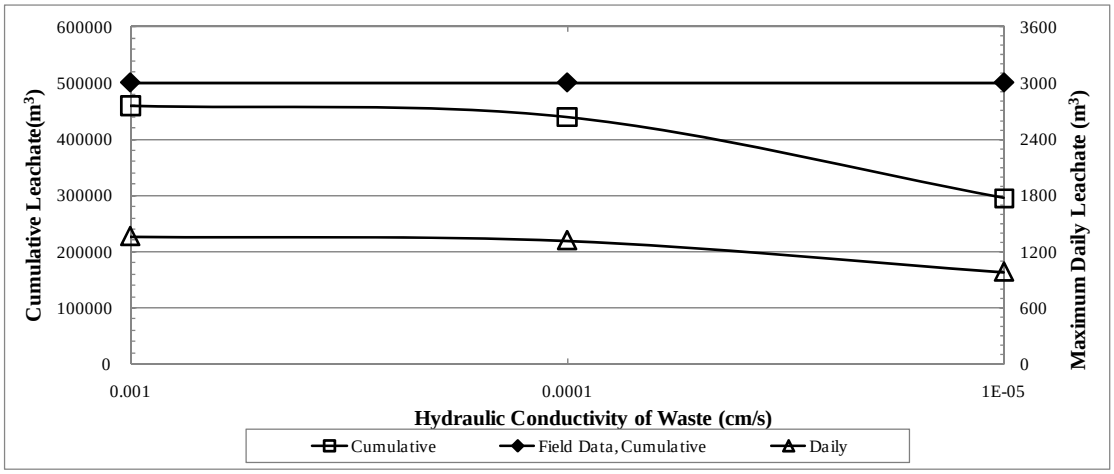

Figure 4-8: Variation of Leachate Production with Hydraulic Conductivity of Waste

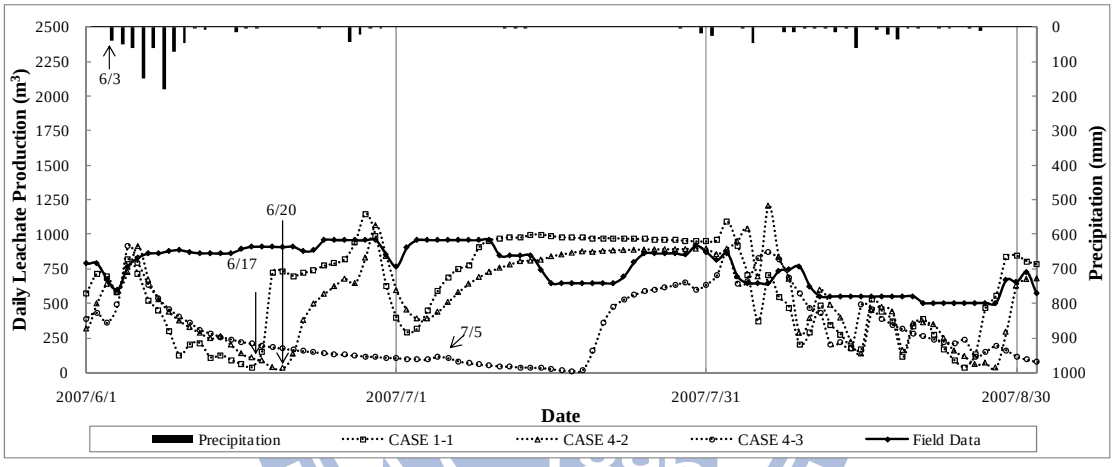

Figure 4-9: Variation of Daily Leachate Production with Hydraulic Conductivity of Waste, between 2007/6/1 and 2007/9/1

Figure 4-10 indicates the loading condition for daily leachate treatment. In 731 days, the loading capacity is above 50% for 728 days in field data and 524 days in CASE 1-1. The daily leachate treatment is in full loaded capacity for 174 days in field data and 253 days in CASE 1-1.

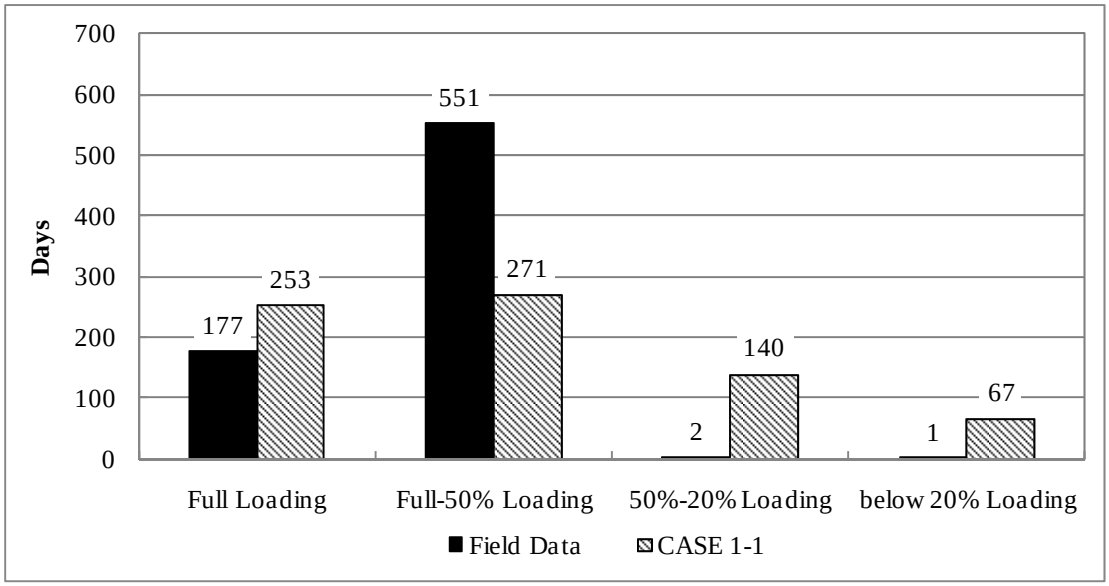

Figure 4-10: Variation of Loading Capacity with Days for Bali Landfill in 731 days

4.1.2 Toufen Landfill

The summary of Visual HELP analysis for Toufen Landfill is listed in Table 4-2.

Table 4-2: Summary of Simulation Result of Toufen Landfill from HELP

	Case 1-1	Case 1-2	Case 1-3	Case 2-1	Case 2-2	Case 2-3	Case 2-4	Case 2-5
Difference (m^3)	63	42	38	61	63	65	66	66
CLP (m^3)	48,675	34,547	26,691	48,618	48,801	48,902	48,926	48,937
MDL (m^3)	250	189	165	235	237	268	286	301
H1 (m)	0.098	0.080	0.073	0.147	0.065	0.024	0.015	0.012
H2 (m)	0.006	0.005	0.004	0.280	0.105	0.039	0.025	0.018
	Case 2-6	**Case 2-7**	**Case 2-8**	**Case 3-1**	**Case 3-2**	**Case 3-3**	**Case 3-4**	**Case 3-5**
Difference (m^3)	66	66	66	63	62	57	58	62
CLP (m^3)	48,711	48,712	48,715	48,675	48,617	47,612	48,392	49,277
MDL (m^3)	295	296	302	250	257	285	218	263
H1 (m)	0.009	0.008	0.007	0.098	0.269	1.436	2.459	2.478
H2 (m)	0.014	0.013	0.012	0.006	0.021	0.161	1.520	2.420
	Case 3-6	**Case 3-7**	**Case 3-8**	**Case 4-1**	**Case 4-2**	**Case 4-3**	**Case 5-2**	**Case 7-2**
Difference (m^3)	62	62	62	63	59	44	87	85
CLP (m^3)	49,058	48,999	48,995	48,675	46,883	35,210	65,295	65,360
MDL (m^3)	260	259	259	250	194	131	248	233
H1 (m)	2.484	2.483	2.483	0.098	0.129	0.102	0.107	0.259
H2 (m)	2.423	2.424	2.425	0.006	0.005	0.004	0.006	0.019
	Case 7-3	**Case 7-4**	**Case 7-5**	**Case 7-6**	**Case 7-7**	**Case 7-8**	**Case 6-1**	**Case 6-2**
Difference (m^3)	81	84	90	90	90	90	84	86
CLP (m^3)	65,218	65,977	66,612	66,605	66,547	66,567	65,292	65,459
MDL (m^3)	240	271	245	248	248	248	210	219
H1 (m)	1.848	3.205	3.261	3.274	3.276	3.276	0.183	0.060
H2 (m)	0.161	1.864	1.958	3.042	3.050	3.051	0.315	0.103
	Case 6-3	**Case 6-4**	**Case 6-5**	**Case 6-6**	**Case 6-7**	**Case 6-8**		
Difference (m^3)	90	91	91	91	91	91		
CLP (m^3)	65635	65674	65693	65704	65706	65711		
MDL (m^3)	233	245	254	261	262	266		
H1 (m)	0.022	0.014	0.010	0.008	0.008	0.007		
H2 (m)	0.036	0.023	0.017	0.014	0.013	0.011		

Difference: Calculated by root mean square method; CLP: Cumulative Leachate Production;
MDL: Maximum Daily Leachate; H1: Highest Leachate Head in Zone 1, similar to H2, H3, etc.

Figure 4-11 shows the cumulative leachate production of the most suitable condition and the field data. The cumulative leachate production is 48,675 m^3 which is 339.9% of field data (20,287 m^3). Among all simulation cases, the minimum difference is 38.385 m^3 which is obtained from CASE 1-3. The cumulative leachate production of CASE 1-3 is 26,691 m^3 which is the closest to the field data.

Figure 4-12 shows that the cumulative leachate production reduces from 48,675 m^3 to 26,691 m^3 while the evaporative depth increases from 3 cm to 30 cm. The daily leachate production is shown in Figure 4-13. Figure 4-14 provides a close observation of daily leachate production between 2007/8/1 and 2007/12/31. It shows that as the evaporation increases, the time lag of leachate production increases to within 4 days. The amount of leachate productions is different among CASE 1-1, CASE1-2, and CASE 1-3, but the production rate is similar in CASE 1-2 and CASE 1-3. While the evaporative depth is less, the leachate production is sensitive to the precipitation.

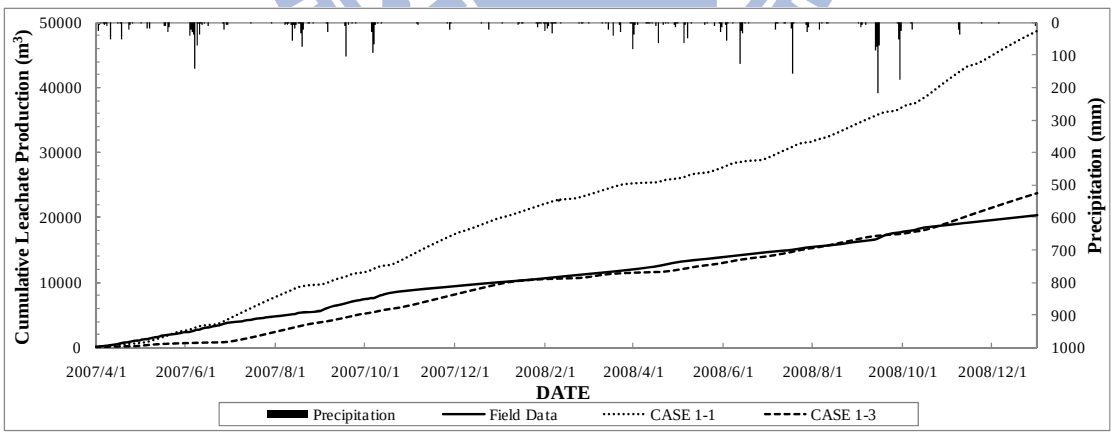

Figure 4-11: Cumulative Leachate Collection

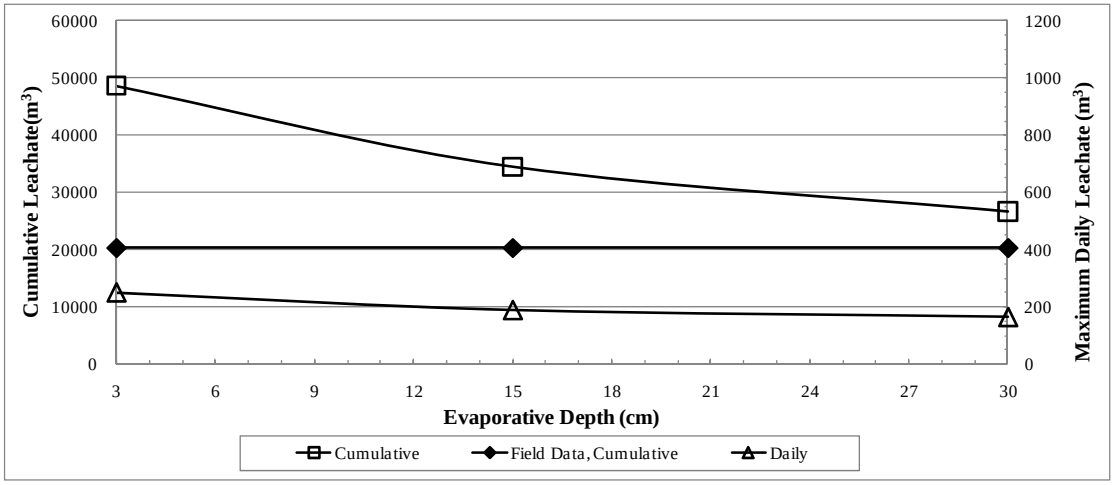

Figure 4-12: Variation of Leachate Production with Evaporative Depth

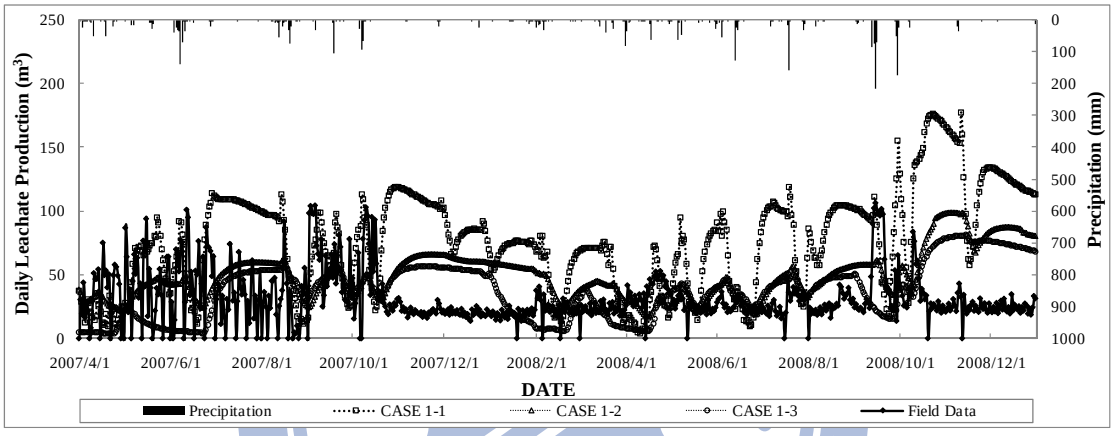

Figure 4-13: Variation of Daily Leachate Production with Evaporative Depth

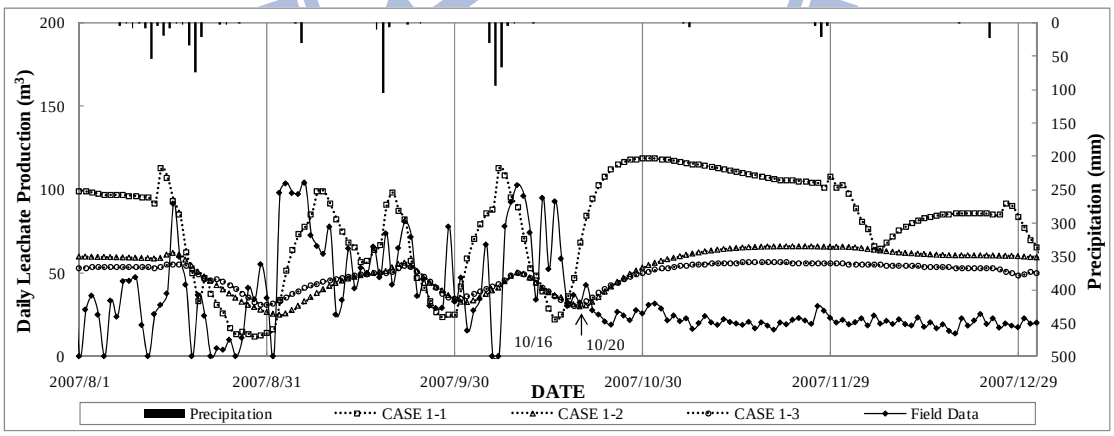

Figure 4-14: Variation of Daily Leachate Production with Evaporative Depth, between 2007/8/1 and 2007/12/31

The variation of leachate production with slope of leachate collection and removal system is shown in Figure 4-15. The cumulative leachate production increases from 48,618 m^3 to 48,936 m^3 when the slope of LCRS increases from 0% to 7%.

Then the increase of leachate production drops to 48,710 m^3 when the slope is 9%. While the slope of LCRS is greater than 7%, the leachate production decreases due to the increase of evaporation. Figure 4-16 shows the variation of leachate production with the change of slope of leachate collection for two heights of waste. When the landfill reaches the designed fill limit (height of waste increases from 20 m to 37 m), the cumulative leachate production increases to 65,294 m^3. As the height of waste is 20 m, the evaporation does increase while the slope of LCRS is greater than 7% in CASE 2 hence the cumulative leachate production reduces. But the evaporation does not increase as the height of waste increases to 37 m. Therefore the increase of evaporation as the height of waste is an error in HELP.

Figure 4-17 shows that the highest leachate head becomes low while the slope of LCRS increases.

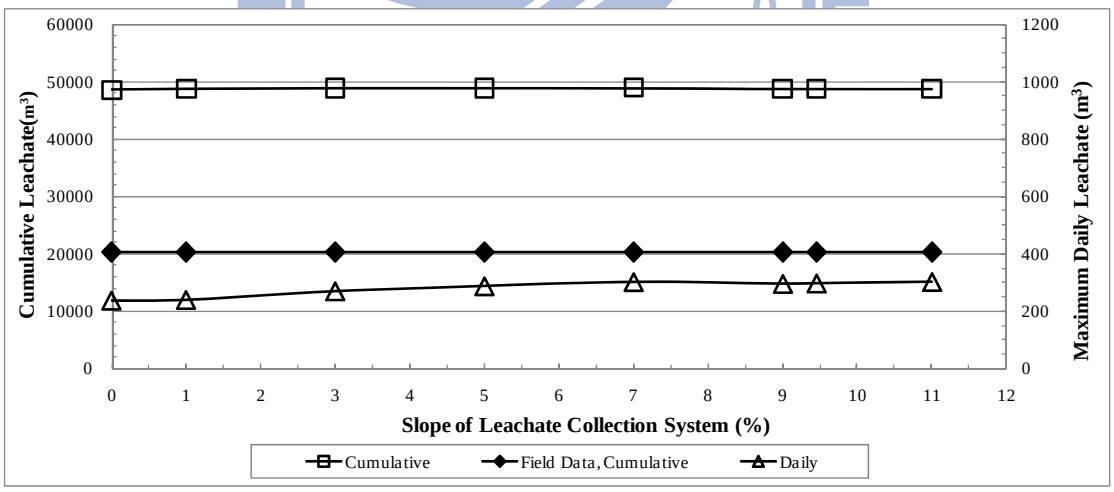

Figure 4-15: Variation of Leachate Production with LCRS Slope

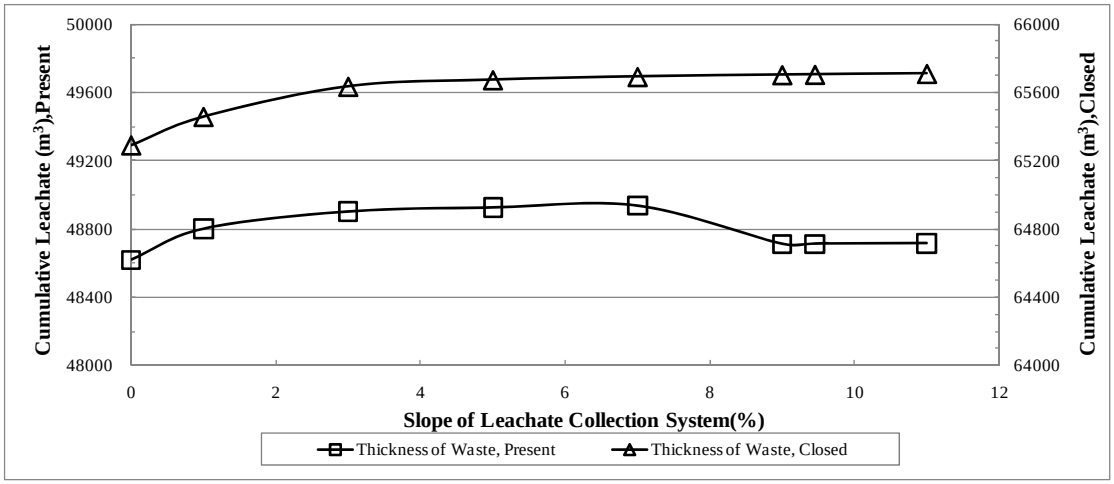

Figure 4-16: Variation of Leachate Production with LCRS Slope and the Height of Waste

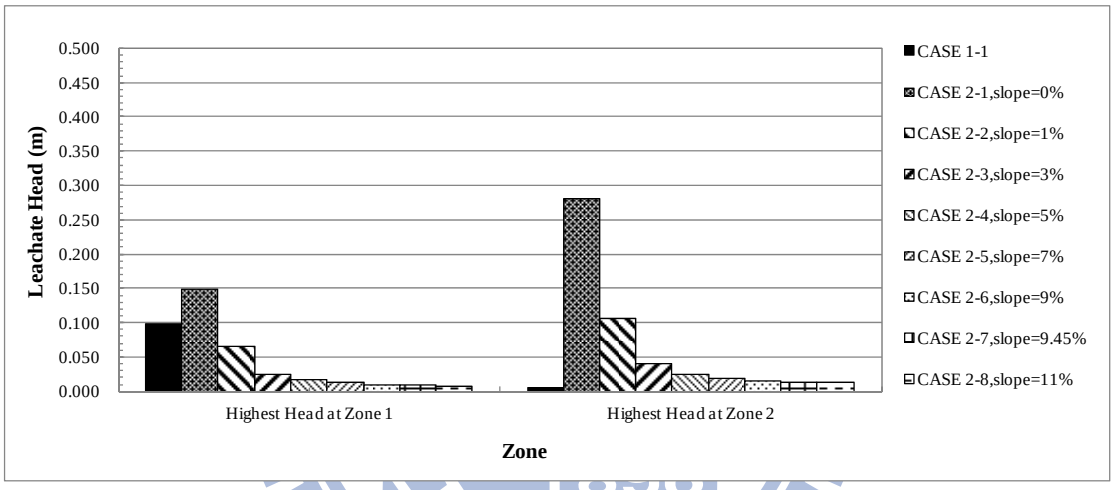

Figure 4-17: Variation of Leachate Head with LCRS Slope

Figure 4-18 shows the variation of cumulative leachate production and highest leachate head with hydraulic conductivity of LCRS. The difference of cumulative leachate production ranges within 1,062 m^3. In Figure 4-19, while the landfill reaches the designed fill limit, the difference of cumulative leachate production ranges within 1,318 m^3. With the increase of waste, both the cumulative leachate production and leachate head increases. While the waste layer reaches the design fill limit, the area of landfill increases from 21,618 m^2 to 29,360 m^2. As a result, the more precipitation infiltrates into the landfill, the more leachate is produced. Figure 4-20 shows the variation of daily leachate production with height of waste layer. The curve of daily lea-

chate production of CASE 1-1 is similar to CASE 5-1 and the only difference is the quantity of leachate production.

Figure 4-21 shows that the cumulative leachate production decreases from 48,675 m^3 to 35,210 m^3 while the hydraulic conductivity of waste decreases from 1×10^{-3} cm/s to 1×10^{-5} cm/s. Meanwhile, the maximum daily leachate production reduces from 250 m^3 to 131 m^3. The low hydraulic conductivity of waste cause the vertical flow rate to decrease hence less leachate products and the leachate head rises.

Figure 4-22 indicates the variation of daily leachate production of CASE 4 group. After the rainfall on 10/5, the decreasing leachate production increases again on October 16 in CASE 1-1. Therefore the time lag of CASE 1-1 is 11 days. The time lag of leachate production increases while the hydraulic conductivity of waste decreases. The time lag of leachate production increases from 11 days to 13 days in CASE 4-2 and to 30 days in CASE 4-3.

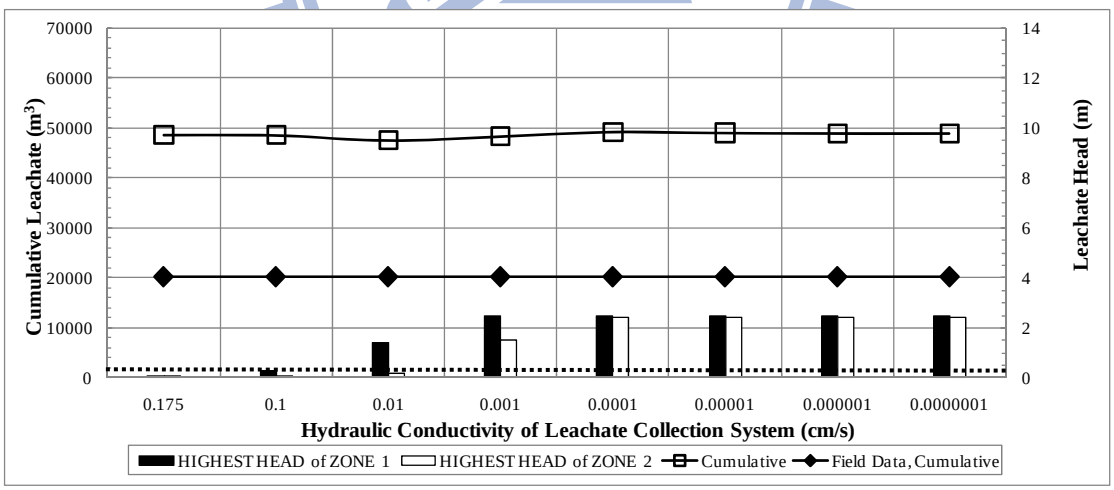

Figure 4-18: Variation of Leachate Production and Leachate Head with Hydraulic Conductivity of LCRS, Present

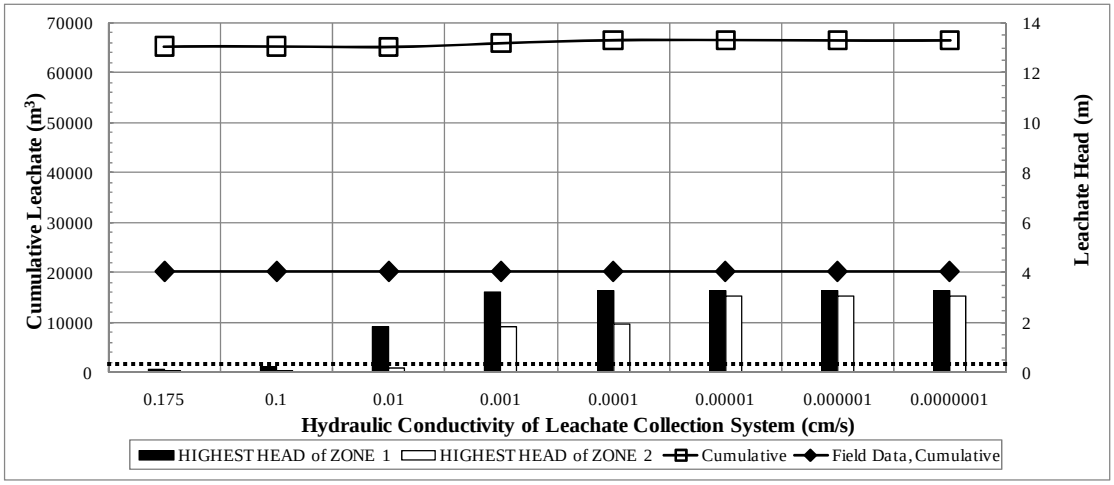

Figure 4-19: Variation of Leachate Production and Leachate Head with Hydraulic Conductivity of LCRS, Closed

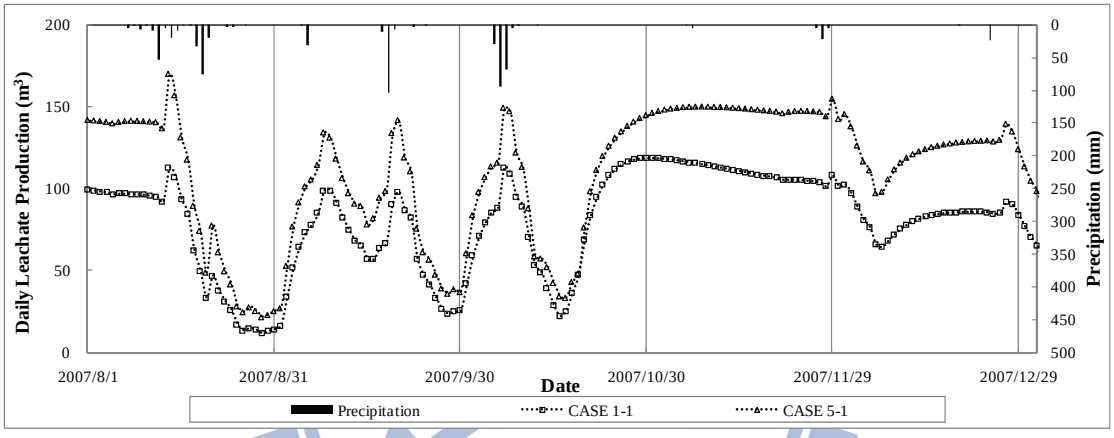

Figure 4-20: Variation of Daily Leachate Production with Height of Waste, Close Observation

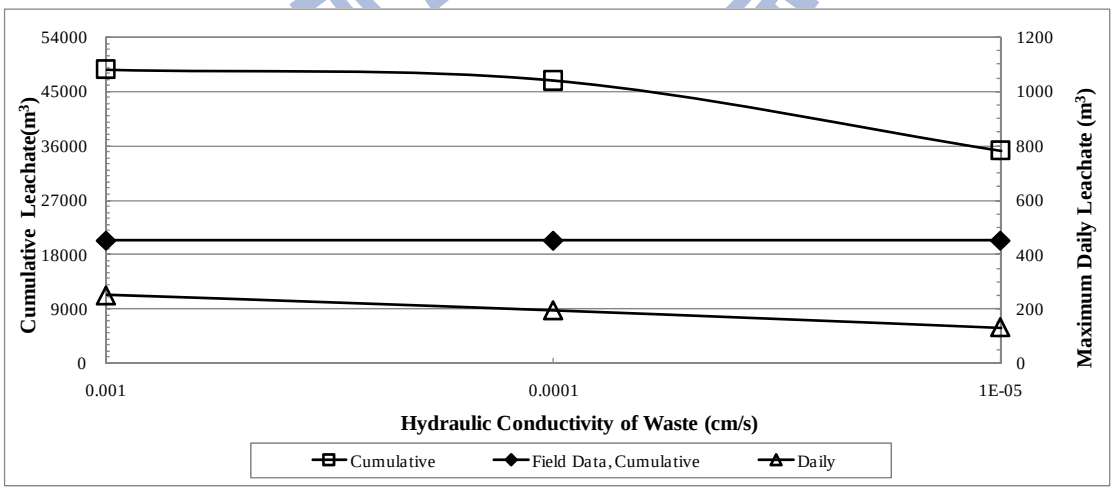

Figure 4-21: Variation of Leachate Production with Hydraulic Conductivity of Waste

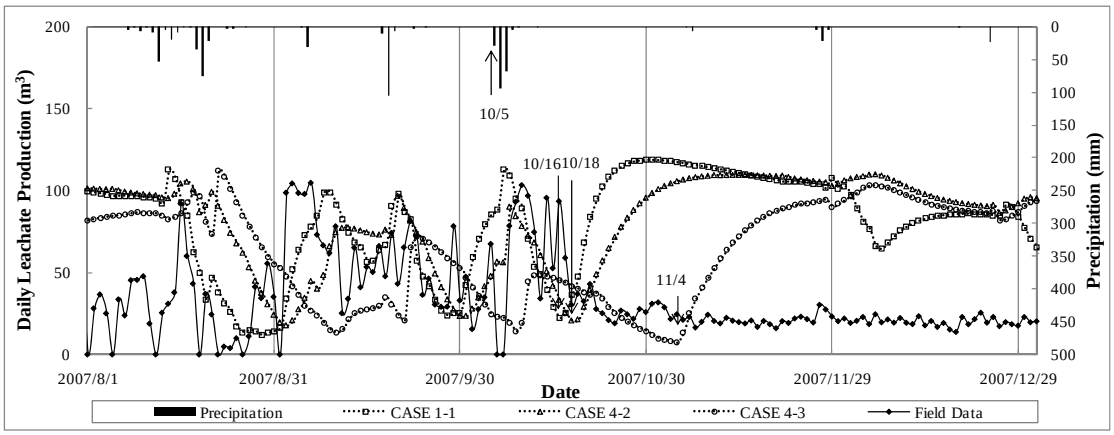

Figure 4-22: Variation of Daily Leachate Production with Hydraulic Conductivity of Waste, Close Observation

Figure 4-23 indicates the loading condition for daily leachate treatment. In 641 days, the loading capacity is below 50% for all the days in field data and for 584 days in CASE 1-1. The daily leachate treatment is in full loaded capacity for 0 days in field data and in CASE 1-1. Hence the design maximum daily leachate treatment is much greater than the simulation and field data.

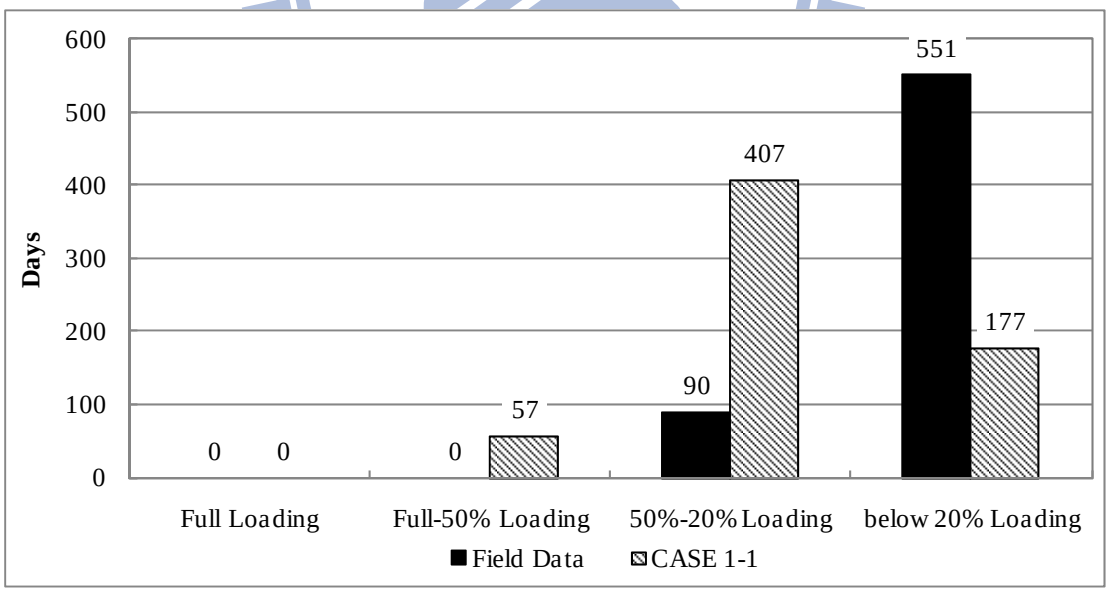

Figure 4-23: Variation of Loading Capacity with Days for Toufen Landfill in 641 days

4.1.3 Anding Landfill

The summary of Visual HELP analysis for Toufen Landfill is listed in Table 4-3

Table 4-3: Summary of Simulation Result of Anding Landfill from HELP

	Case 1-1	Case 5-2	Case 5-3	Case 1-1	Case 1-2	Case 1-3	Case 1-1	Case 3-2
Difference (m^3)	174	176	276	174	145	131	174	170
CLP (m^3)	128,988	128,723	128,780	128,988	97,065	83,684	128,988	128,339
MDL (m^3)	1,610	2,530	1,862	1,610	1,408	1,343	1,610	1,573
H1 (m)	4.23	4.80	2.72	4.23	3.95	3.87	4.23	4.23
	Case 3-3	**Case 3-4**	**Case 3-5**	**Case 3-6**	**Case 3-7**	**Case 3-8**	**Case 4-1**	**Case 4-2**
Difference (m^3)	166	169	171	168	172	173	174	117
CLP (m^3)	125,626	124,374	127,394	122,002	127,967	129,081	128,988	131,382
MDL (m^3)	1,555	1,574	1,585	1,568	1,586	1,589	1,610	450
H1 (m)	4.23	4.27	4.29	4.26	4.29	4.29	4.23	5.60
	Case 4-3	**Case 4-4**	**Case 7-1**	**Case 7-2**	**Case 7-3**	**Case 7-4**	**Case 7-5**	**Case 7-6**
Difference (m^3)	104	94	176	174	172	173	175	172
CLP (m^3)	122,195	72,331	128,723	128,115	125,208	124,382	127,217	122,310
MDL (m^3)	234	211	2,530	2,502	2,493	3,032	2,513	2,492
H1 (m)	5.60	5.60	4.80	4.80	4.80	5.95	4.83	4.80
	Case 7-7	**Case 7-8**	**Case 9-1**	**Case 9-2**	**Case 9-3**	**Case 9-4**	**Case 9-5**	**Case 9-6**
Difference (m^3)	176	175	276	275	274	280	285	283
CLP (m^3)	127,660	128,709	128,780	128,234	125,453	124,940	128,324	124,088
MDL (m^3)	2,515	3,001	1,862	1,860	1,853	1,862	1,858	1,858
H1 (m)	4.83	5.92	2.72	2.72	2.72	2.72	2.69	2.72
	Case 9-7	**Case 9-8**	Difference: Calculated by root mean square method;					
Difference (m^3)	285	287	CLP: Cumulative Leachate Production;					
CLP (m^3)	128,072	128,831	MDL: Maximum Daily Leachate;					
MDL (m^3)	1,861	1,866	H1: Highest Leachate Head in Zone 1, similar to H2, H3, etc.					
H1 (m)	2.69	2.70						

Figure 4-25 shows the cumulative leachate production of the most suitable condition and the field data. The result of CASE 1-1 is over the field data while the cumulative leachate production is 128,988 m^3. Among all cases, the minimal difference is 94.3 m^3 which is obtained from CASE 4-7. On the other hand, cumulative leachate production of CASE 1-3 is 83,684 m^3 and approaches the field data the most.

Figure 4-25 shows the leachate production with evaporative depth. The cumulative leachate production decreases from 128,988 m^3 to 83,684 m^3 as the evaporative depth increases from 3 cm to 30 cm. In the mean time, the maximum daily leachate production decreases from 1,610 m^3 to 1,342 m^3.

Figure 4-26 provides a close observation to the daily leachate production with evaporative depth. The evaporative depths of CASE 1-1, CASE 1-2, and CASE 1-3 are 3 cm, 15 cm, and 30 cm respectively. The amount of the leachate production is different among CASE 1-1 to CASE 1-3 but the leachate production rate is the same. The daily leachate production of CASE 1-2 and CASE 1-3 is all below 100 m^3 from 6/1 to 8/10 and sometimes is below 50 m^3. In the same time, the daily leachate production of CASE 1-1 is over 100 m^3 in some days. After 8/9, the daily leachate production is affected by the rainfall from 8/9 to8/22. The leachate production starts to rise on 8/13. The time lag of leachate production is similar to each other. Due to the increase of evaporation, CASE 1-2 and CASE 1-3 is not as sensitive to the precipitation as CASE 1-1. It can be seen that while the evaporative depth is as shallow as 3 cm, the leachate production is more sensitive to the precipitation.

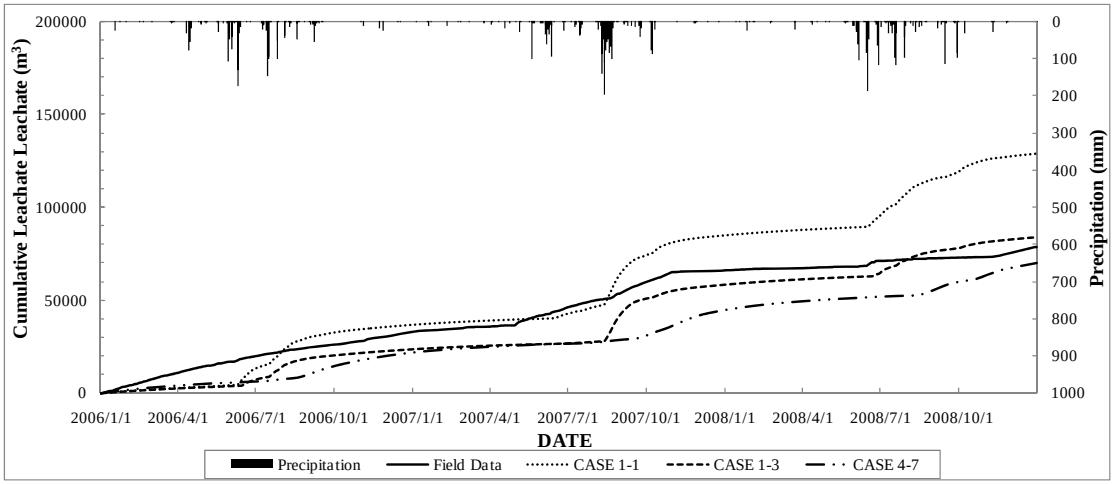

Figure 4-24: Cumulative Leachate Collection

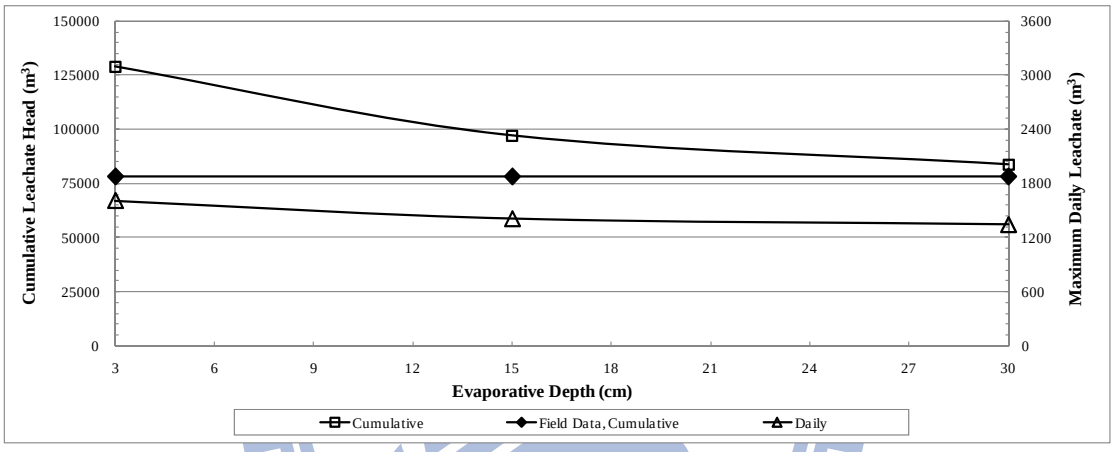

Figure 4-25: Variation of Leachate Production with Evaporative Depth

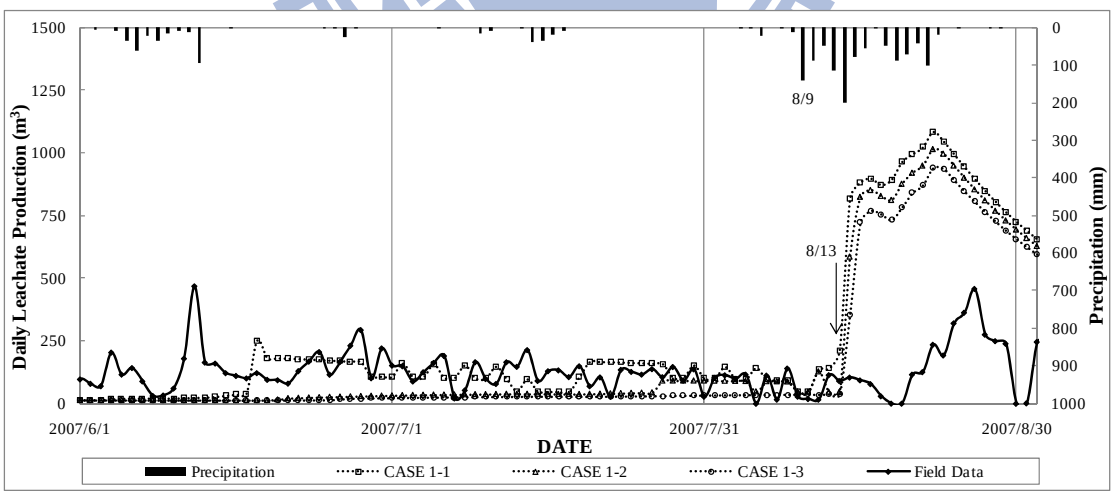

Figure 4-26: Variation of Daily Leachate Production with Evaporative Depth, between 2007/6/1 and 2007/9/1

Figure 4-27 shows the variation of leachate production with the height of waste.

The difference of cumulative leachate production ranges within 265 m^3 hence the change of height of waste only causes extremely small change to the cumulative leachate production. On the other hand, daily leachate production first rises from 1,610 m^3 to 2,530 m^3 in CASE 5-2 (the height of waste is 12.6 m), and then reduces to 1,862 m^3 in CASE 5-3 (the height of waste is 25.1 m). Figure 4-28 shows that the daily leachate production increases while the height of waste increases. The evaporation in CASE 1-1, CASE 5-2, and CASE 5-3 is all the same hence the evaporation is not affected by the height of waste.

The maximum daily leachate production in CASE 5-2 is an exceptional case. The maximum daily leachate (2,530 m^3) in CASE 5-2 occurs on 1994/8/16.The daily leachate production is shown in Figure 4-30 and the leachate head is shown in Figure 4-31. Due to the precipitation since8/3 to 8/15, the leachate production rate increases after 8/9. It can be seen that the leachate production rate of CASE 5-2 is suddenly greater than CASE 5-3 on 8/16 and 8/17 and lower than CASE 5-3 after 8/18. The height of waste in CASE 5-2 is not thick enough to provide a buffer for draining out all the leachate. Before the leachate is drained out, the additional leachate also reaches the bottom of waste layer. Therefore, the leachate head rises and the leachate production increases.

In CASE 5-3, the height of waste layer provides a long path for the vertical flow of leachate and can be considered as a better buffer. The leachate head and daily leachate production in CASE 5-3 are all smaller than in CASE 5-2.

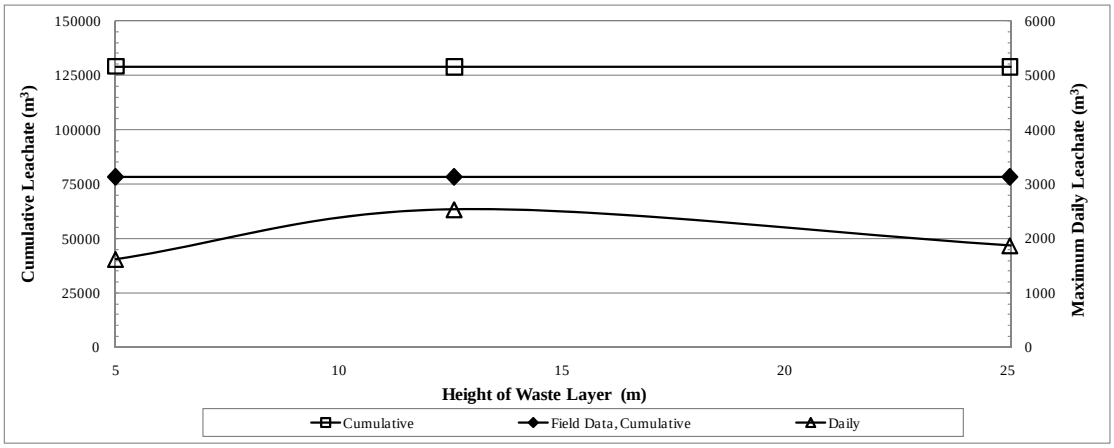

Figure 4-27: Variation of Leachate Production with Height of waste

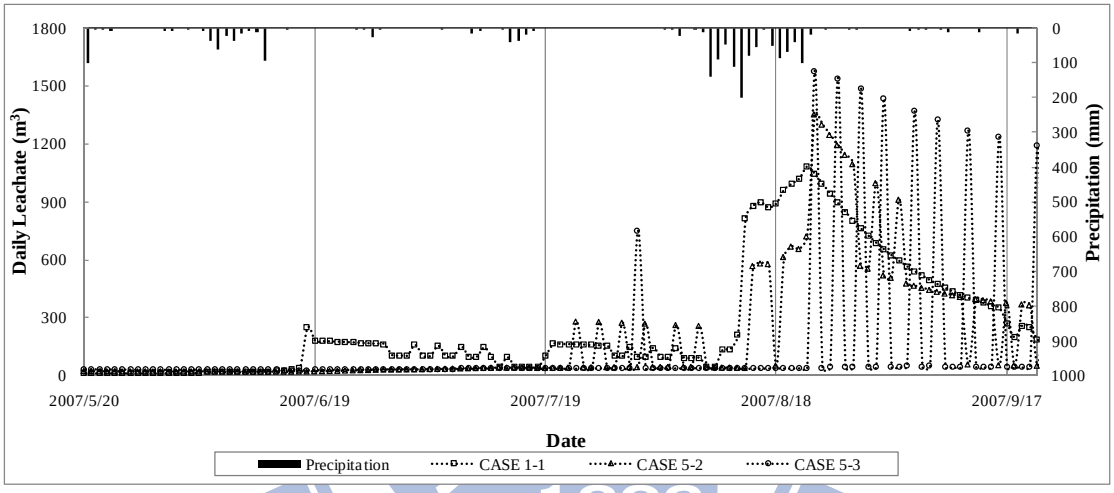

Figure 4-28: Variation of Daily Leachate Production with Height of waste, between 2007/5/20 and 2007/9/20

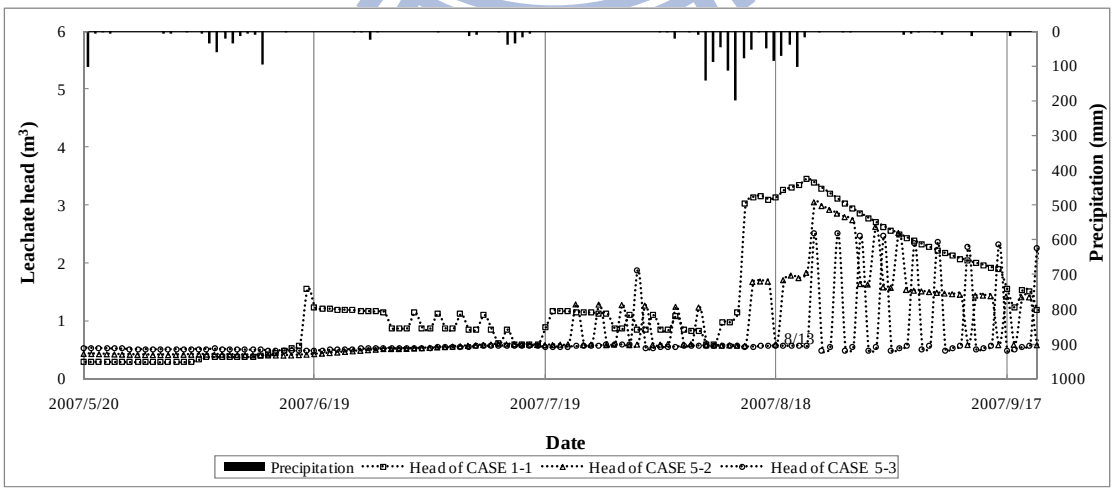

Figure 4-29: Variation of Daily Leachate Head with Height of waste, Close Observation

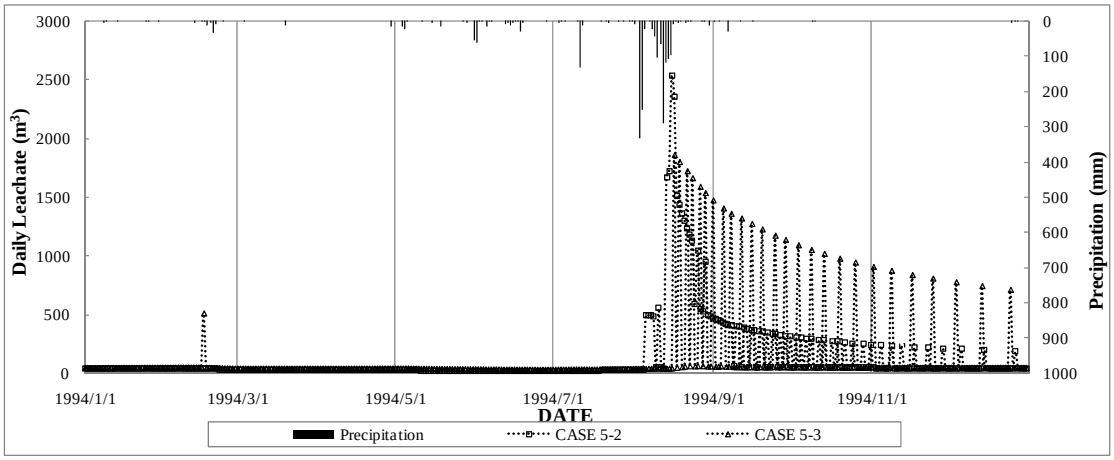

Figure 4-30: Variation of Daily Leachate Production with Height of waste in 1994

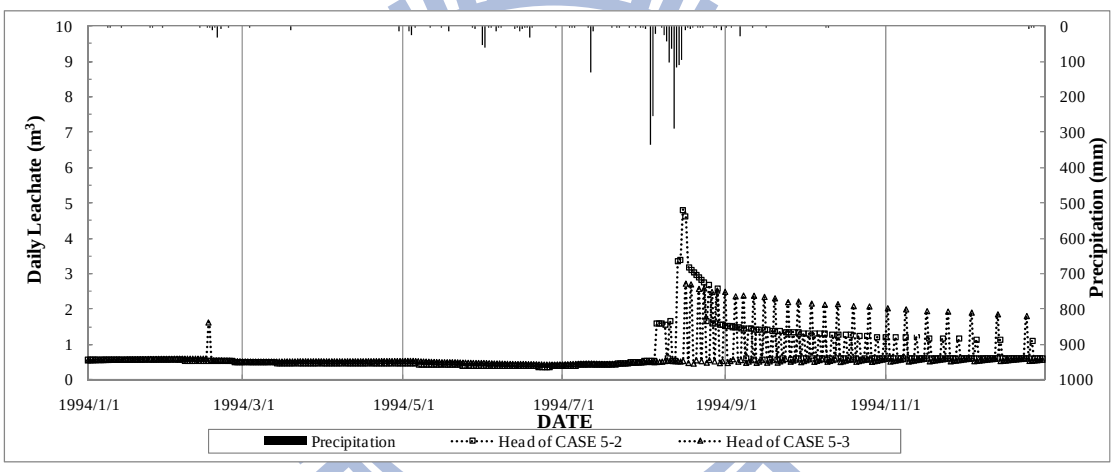

Figure 4-31: Variation of Leachate Head with Height of Waste in 1994

Figure 4-32 shows the variation of cumulative leachate production and leachate head with the height of waste and hydraulic of LCRS. First of all, the cumulative leachate is almost the same in 3 series of case (CASE 3, CASE 7, CASE 9). Though the height of waste increases, the cumulative leachate production does not change much. The leachate head should decrease with the increase of the height of waste while the height of waste provides a buffer for draining out the leachate. But in the series of CASE 7, the leachate production and leachate head rise rapidly August 14, 1994. Therefore, the highest leachate head in the series of CASE 7 is higher than of CASE 3

and CASE 9.

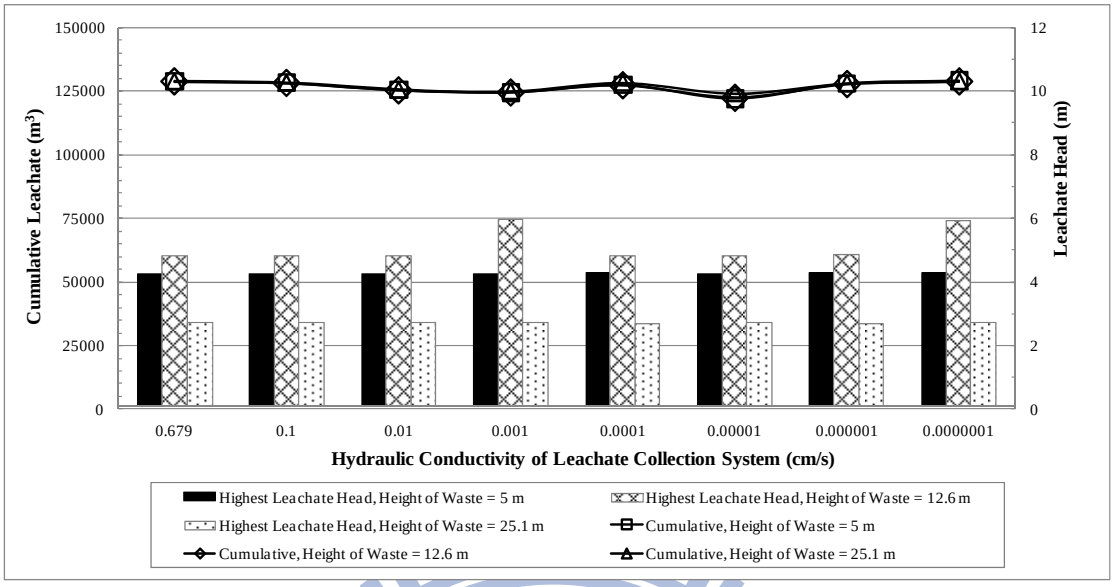

Figure 4-32: Variation of Cumulative Leachate Production and Highest Leachate Head with the Height of Waste and Hydraulic Conductivity of LCRS

As indicated in Figure 4-33, the leachate production decreases with the decrease of the hydraulic conductivity of waste. While the hydraulic conductivity decreases from 1×10^{-2} cm/s to 1×10^{-5} cm/s, the daily leachate production decreases from 1,610 m^3 to 211 m^3. Due to the decrease of hydraulic conductivity of waste, the leachate head rises and less leachate is produced. Figure 4-34 shows the time lag of leachate production with hydraulic conductivity of waste. With the increase of hydraulic conductivity of waste, the time lag of leachate production increases from 4 days to 26 days. Moreover, the daily leachate production is become less sensitive to the precipitation with the decrease of hydraulic conductivity of waste. The leachate production rate increases rapidly with precipitation when the hydraulic conductivity of waste is as high as 0.01 cm/s. Along with the decrease of hydraulic conductivity of waste, the curve of the daily leachate production becomes smoother.

Figure 4-35 illustrates that maximum leachate head increases with the decrease

of the hydraulic conductivity of waste. The leachate head increases with the decrease of hydraulic conductivity. Hence the cumulative leachate production decreases.

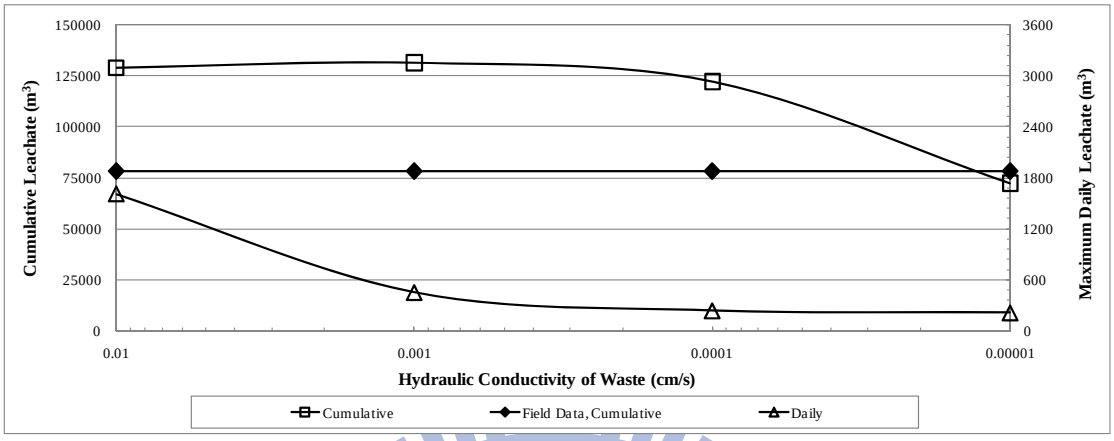

Figure 4-33: Leachate Production with Hydraulic Conductivity of Waste

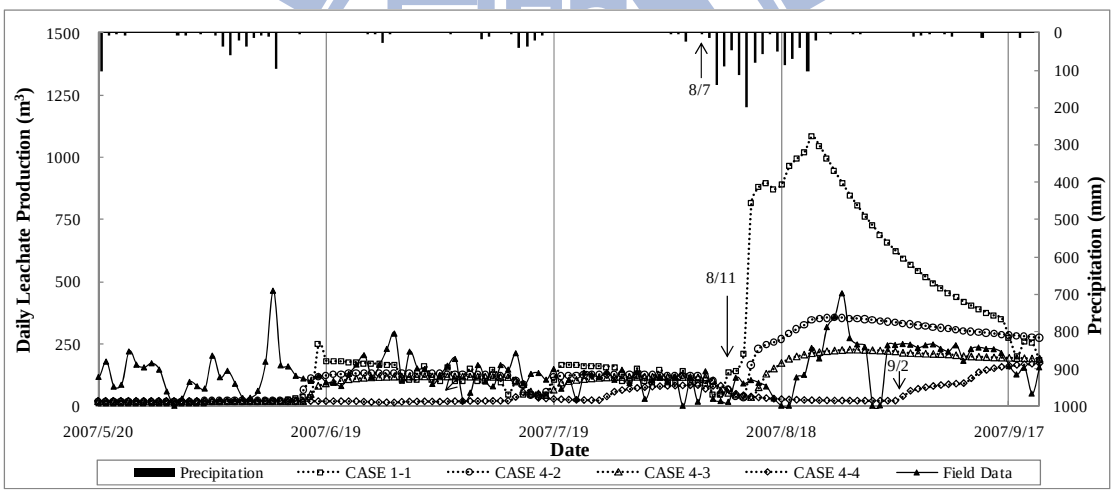

Figure 4-34: Variation Daily Leachate Production with Hydraulic Conductivity of Waste, between 2007/5/20 and 2007/9/20

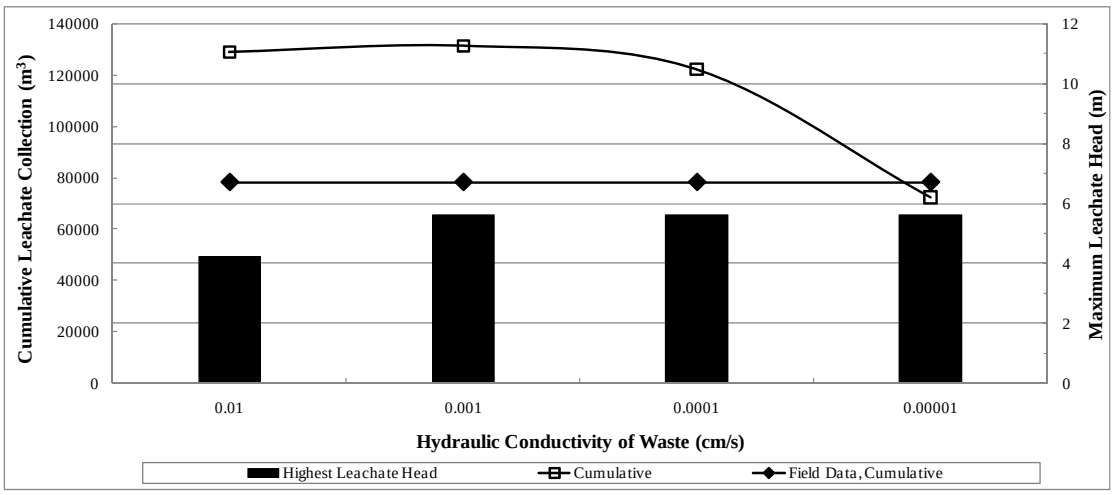

Figure 4-35: Variation Leachate Production and Leachate Head with Hydraulic Conductivity of Waste, Closed

Figure 4-36 indicates the loading condition for daily leachate treatment. In 1096 days, the loading capacity is below 50% for 1,084 days in field data and 957 days in CASE 1-1. The daily leachate treatment is in full loaded capacity for 0 day in field data and 20 days in CASE 1-1.

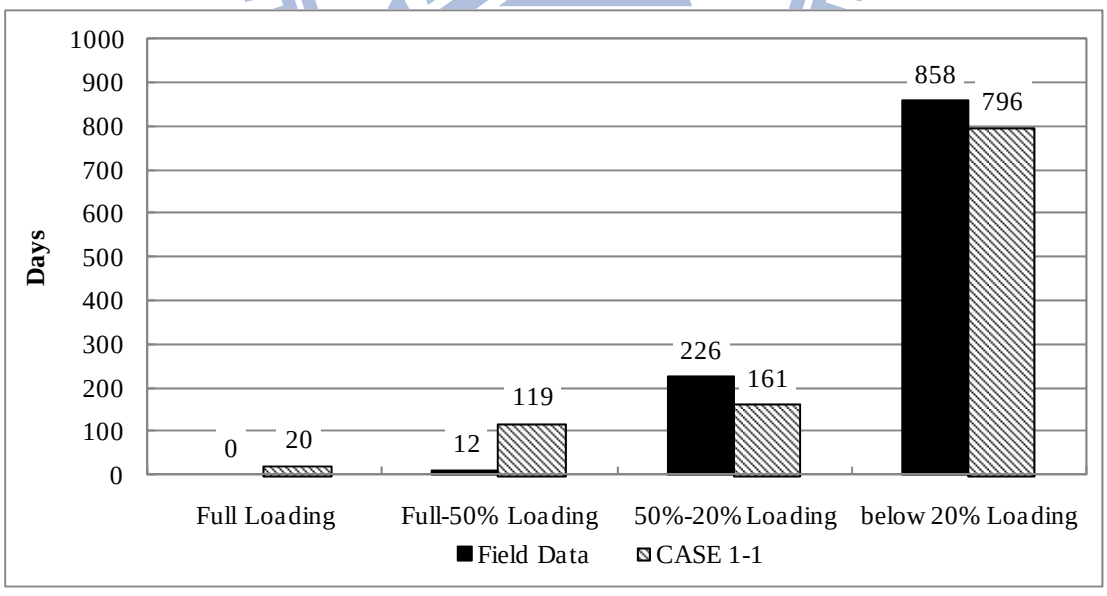

Figure 4-36 : Variation of Loading Capacity with Days for Anding Landfill in 731 days

4.2 Slope Stability Analysis

4.2.1 Bali Landfill

The result of factor of safety obtained from slope stability analysis in Bali Landfill is shown in Figure 4-37 and Table 4-4. The factor of safety decreases from 3.52 to 3.15 when the hydraulic conductivity of LCRS decreases from 0.175 cm/s to 1×10^{-7} cm/s. As mentioned in section 4.1, the leachate head will rise as the hydraulic conductivity of LCRS decreases. Therefore, the factor of safety approaches 3.2 as the leachate tends to be stable when the hydraulic conductivity of LCRS is below 1×10^{-4} cm/s. In the same condition, as the interfacial friction angle reduces to 8°, the factor of safety decreases from 1.85 to 1.66.

As the failure surface is located automatically, the shape of slip surface is found to be as an over-turned trapezoid. When the hydraulic conductivity of LCRS decreases from 0.175 cm/s to 1×10^{-7} cm/s, the factor of safety decrease from 2.78 to 2.66 and 2.50 to 2.45 as the interfacial friction angle is 15° and 8°, respectively. It can be seen that the result of auto-located failure surface are not consistent with the translational failure.

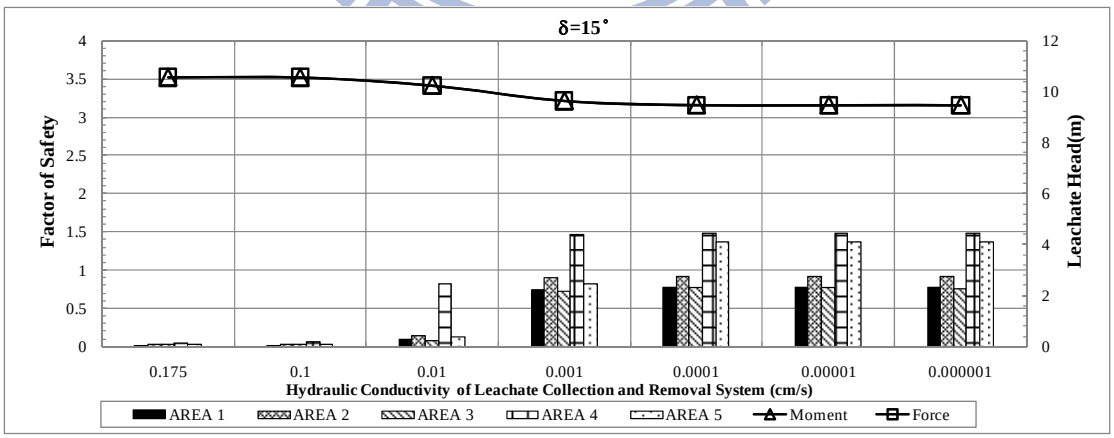

Figure 4-37: Variation Factor of Safety with Hydraulic Conductivity of Leachate collection and removal system, with the interfacial friction angle as 15°

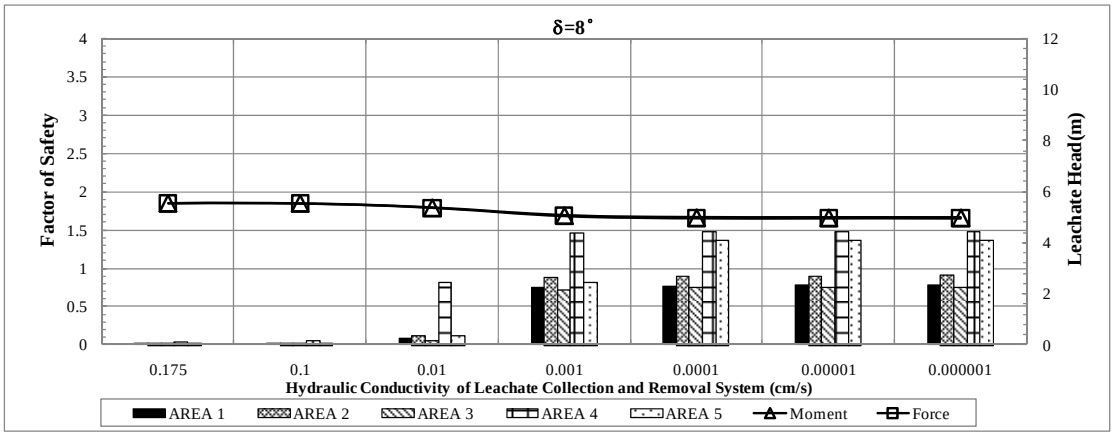

Figure 4-38: Variation Factor of Safety with Hydraulic Conductivity of Leachate collection and removal system, with the interfacial friction angle as 8°

Table 4-4: Factor of Safety obtained from Slope Stability Analysis

Hydraulic Conductivity of LCRS		0.175	1×10^{-1}	1×10^{-2}	1×10^{-3}	1×10^{-4}	1×10^{-5}	1×10^{-6}	1×10^{-7}
δ = 15°	Moment	3.518	3.516	3.410	3.210	3.156	3.154	3.153	3.153
	Force	3.518	3.516	3.410	3.210	3.156	3.154	3.153	3.153
δ = 8°	Moment	1.854	1.853	1.796	1.691	1.664	1.662	1.662	1.662
	Force	1.845	1.844	1.788	1.683	1.655	1.654	1.654	1.654

4.2.2 Toufen Landfill

The factor of safety obtained from slope stability analysis is shown in Figure 4-39 to Figure 4-42.The interfacial friction angle between GCL and geomembrane is 15° in Figure 4-39 and Figure 4-40, and 8° in Figure 4-41 and Figure 4-42, respectively.

As the height of waste is 20 m, the factor of safety decreases from 5.97 to 5.20 with the decrease of hydraulic conductivity of LCRS (Figure 4-39). As the height of waste is 37 m, the factor of safety decreases from 2.65 to 2.46 with the decrease of hydraulic conductivity of LCRS (Figure 4-40).

As the interfacial friction angle reduces to 8, the factor of safety decreases dramatically. The factor of safety decreases from 3.13 to 2.73 with the increase of lea-

chate head when the height of waste is 20 m (Figure 4-41). While the height of waste rises to 37 m, the factor of safety decreases from 1.42 to 1.32 with the increase of leachate head (Figure 4-42).

Among the height of leachate head, the height of waste, and the interfacial friction angle between GCL and geomembrane, interfacial friction angle between GCL and geomembrane is most critical to the factor of safety. For example, for the LCRS with hydraulic conduction of 0.3345 cm/s and 20 m of height of waste, the factor of safety drops from 5.97 to 3.13 as the interfacial friction angle decreases from 15° to 8°. Under the same condition, when the height of waste is 37 m, the factor of safety drops from 2.65 to 1.42. On the other hand, for the LCRS with hydraulic conduction of 0.3345 cm/s and 15° of the interfacial friction angle, the factor of safety drops from 5.97 to 2.65 as the height of waste increases from 20 m to 37 m. Under the same condition, when the interfacial friction angle is 8°, the factor of safety drops from 3.13 to 1.42. Thus, the effect of reduction of interfacial friction angle on lowering factor of safety is more significant than that caused by decrease of hydraulic conductivity of LCRS and increase of height of waste.

As the failure surface is located automatically, the shape of slip surface is found to be as an over-turned trapezoid. For the hydraulic conductivity of LCRS decreases from 0.175 cm/s to 1×10^{-7} cm/s and the height of waste is 20 m, the factor of safety decrease from 12.80 to 11.68 and 10.77 to 9.69 as the interfacial friction angle is 15° and 8°, respectively. Under the same condition, for the height of waste is 37 m, the factor of safety decrease from 3.24 to 2.48 whether the interfacial friction angle is 15° or 8°. It can be seen that the result of auto-located failure surface are not consistent with the translational failure and the factor of safety is greater than the failure surface located in the barrier layer.

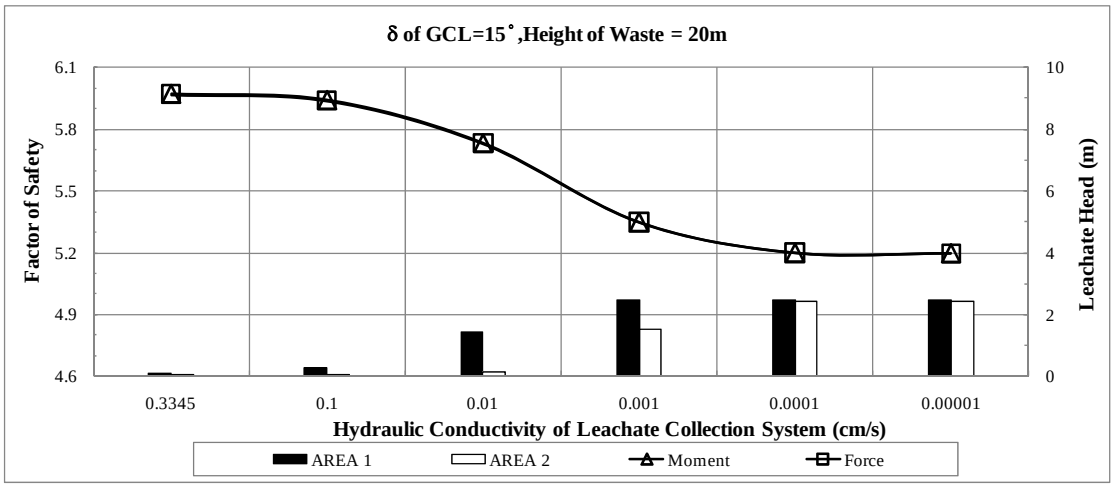

Figure 4-39: Variation Factor of Safety with Hydraulic Conductivity of Leachate collection and removal system, Present

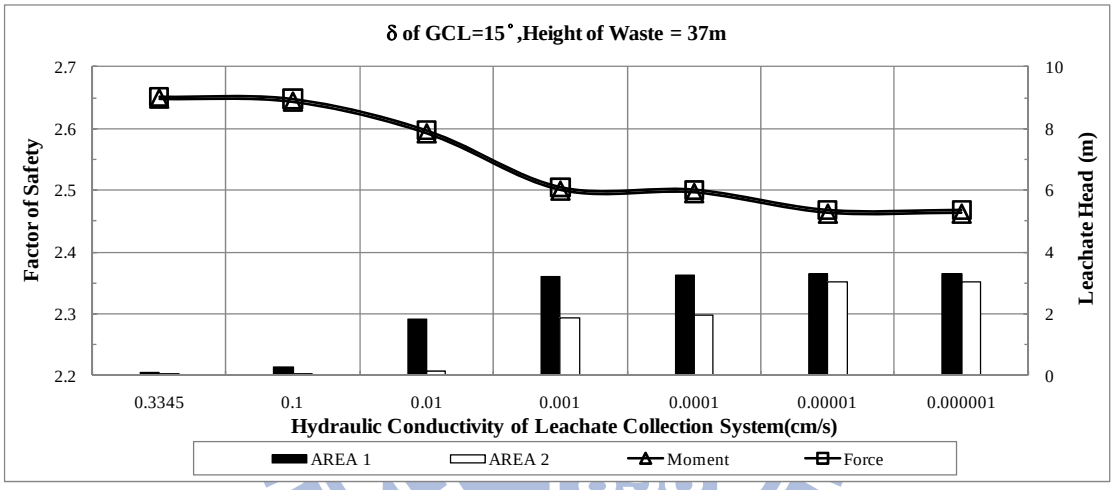

Figure 4-40: Variation Factor of Safety with Hydraulic Conductivity of Leachate collection and removal system, Closed

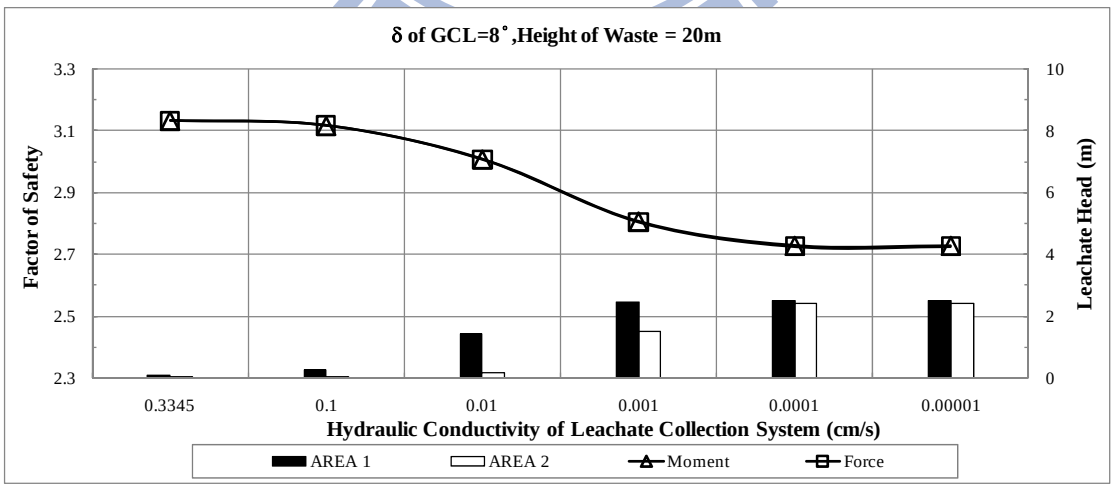

Figure 4-41: Variation Factor of Safety with Hydraulic Conductivity of Leachate collection and removal system, Present, Weak Interface Strength of GCL

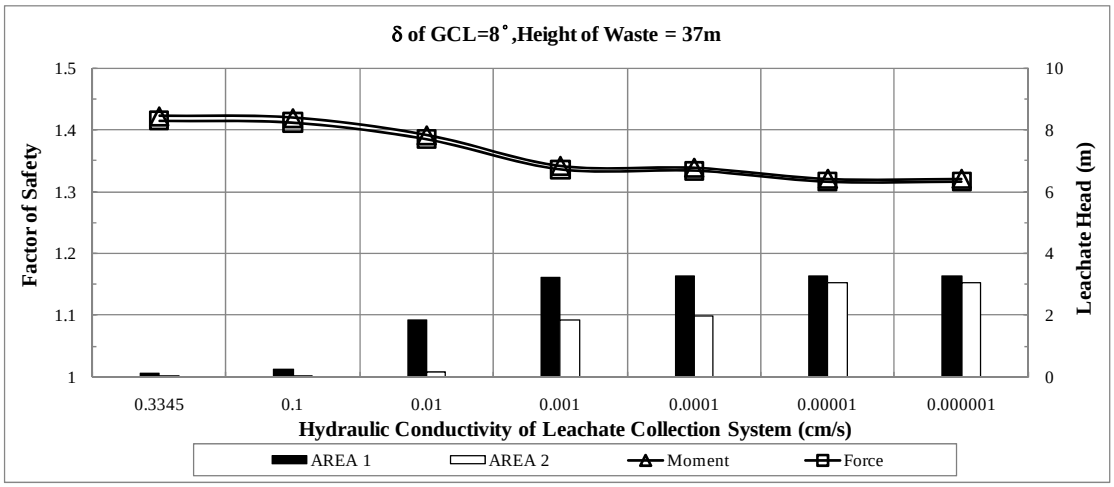

Figure 4-42: Variation Factor of Safety with Hydraulic Conductivity of Leachate collection and removal system, Closed, Weak Interface Strength of GCL

Table 4-5 Summary of Safety of Factor obtained from Slope Stability Analysis in Toufen Landfill

K of LCRS (cm/s)			0.3345	1×10^{-1}	1×10^{-2}	1×10^{-3}	1×10^{-4}	1×10^{-5}	1×10^{-6}
Height of Waste (H=20m)	δ=15°	moment	5.969	5.939	5.730	5.347	5.198	5.196	5.196
		force	5.971	5.941	5.732	5.349	5.200	5.198	5.198
	δ=8°	moment	3.131	3.115	3.006	2.805	2.726	2.726	2.726
		force	3.132	3.116	3.007	2.805	2.727	2.726	2.726
Height of Waste (H=37m)	δ=15°	moment	2.648	2.643	2.592	2.500	2.496	2.463	2.463
		force	2.652	2.648	2.597	2.505	2.501	2.468	2.468
	δ=8°	moment	1.422	1.419	1.391	1.341	1.338	1.320	1.320
		force	1.415	1.412	1.385	1.336	1.334	1.316	1.316

Chapter 5 Summary

5.1 Conclusion

The effect of material properties and design factors on the behavior of LCRS, such as the leachate production rate and cumulative leachate collection is investigated in this study. Furthermore, the resulted leachate head on the slope stability of landfill is assessed. Following conclusions can be drawn from the results:

1. In HELP model, the evaporation of leachate is governed by the evaporative depth. Also, the evaporation affects the quantity of leachate mostly. As the evaporative depth increases for ten times, the cumulative leachate production decreases for about 35% to 45%. Furthermore, with the increase of evaporation, the leachate production is less sensitive to the precipitation.
2. The time lag of leachate production is mainly governed by the hydraulic conductivity of waste. With the increase of hydraulic conductivity of waste, the vertical flow rate decreases. Thus, more leachate is stored in the waste and the height of leachate head rises. The increase of evaporative depth also causes the time lag of leachate production. In comparison with hydraulic conductivity of waste, evaporative depth has less effect to the time lag of leachate production.
3. The increase of height of waste causes the maximum daily leachate to increase. The increase of height of waste provides a thicker buffer for leachate to percolate. With the long distance for leachate to percolate, the leachate is able to be drained out in more time when reach the leachate collection and removal system. Moreover, with the decrease of accumulated leachate head, the daily leachate production increases.

4. The slope of leachate collection and removal system will affect the leachate collection and leachate head. The increase of slope of LCRS will accelerate the production of leachate and decrease the height of leachate head.
5. The decrease of hydraulic conductivity of LCRS will cause the increase of leachate head. With the decrease of hydraulic conductivity of LCRS, the drainage rate of leachate production decreases. Therefore, the leachate accumulated on the barrier layer increases.
6. The leachate production is affected by the leachate head. The computation of lateral drainage will include the hydraulic conductivity of waste when the height of leachate head is over the top of LCRS. Hence, the leachate collection rate will be stable once the increase of hydraulic conductivity of LCRS is smaller than the hydraulic conductivity of waste for more than one order of magnitude.
7. With the increase of leachate head, the factor safety obtained from slope stability analysis of landfill decreases. It is consistent with the result of simulation on slope stability of landfill (Lee, 2008).
8. In comparison with the effect by height of leachate head or height of waste, the effect by the interfacial shear strength between geosynthetics is more critical to the slope stability of landfill. The decrease of friction angle of interfacial shear strength will cause the factor of safety to decrease significantly.
9. The result of water balance analysis of the three landfills shows that the computed leachate production in the most suitable condition can be than the designed quantity of maximum daily leachate treatment after heavy rain. The leachate production rate by HELP during rainy season is always greater

than the designed capacity of leachate treatment plant. During the simulation time for 20 years, for Toufen Landfill, the maximum daily leachate production is found to be greater than the designed quantity of treatment by only 0.8 CMD. On the other hand, for Bali Landfill and Anding Landfill, the maximum daily leachate production is found to be greater than the design quantity of treatment by more than 500 CMD

5.2 Recommendation

In this study, the leachate collection and leachate head are obtained from simulation. The field data does not fully verify the simulation due to quality of field data. For verifying the simulation by field data, the recommendation is listed below:

1. Currently, the leachate head is not monitored in Taiwan's landfill. Leachate head should be monitored to provide vital information for enhancing efficiency of leachate treatment and status of slope stability of the landfill.
2. The rational method currently used for estimating leachate production and, in turn, the capacity of leachate treatment plant did not take into account the properties of the waste and LCRS, and thus often lead to significant over- or under-design of the capacity of leachate treatment plant. Based on the result of this study, it is suggested that the leachate water balance analysis should be performed for the design of LCRS and capacity of leachate treatment plant. In addition, the capacity of LCRS and leachate treatment plant can be optimized for maximum allowable leachate head and cost efficiency of leachate treatment by performing water balance analysis

3. In this study, the number and size of pinholes of the geomembrane liner, hydraulic properties of the waste, and the hydraulic conductivity of LCRS are all assumed based on values obtained from the literature and best estimation. Future study using real values by field investigations is warranted in order to further assess the accuracy and feasibility of leachate water balance analysis.

Reference

Albright, W.H., G.W. Gee, G.V. Wilson, and M.J. Fayer (2002) "Alternative Cover Assessment Project Phase I Report," Desert Research Institute, University and Community College System of Nevada.

Benson, C.H., and X.D. Wang (1998) "Soil Water Characteristic Curves For Solid Waste," *Environmental Geotechnics Report 98-13*. Madison, Wisconsin 53706: Dept. of Civil and Environmental Engineering, University of Wisconsin-Madison.

Berger, K., S. Melchior, and G. Miehlich (1996) "Suitability of Hydrologic Evaluation of Landfill Performance (HELP) model of the US Environmental Protection Agency for the simulation of the water balance of landfill cover systems," *Environmental Geology*, Vol. 28, No. 4, pp 181-189.

Boussinesq, J. (1904) "Recherches théoriques sur l'écoulement des nappes d'eau infiltrées dans le sol; compléments," *Journal de Mathématiques Pures et Appliquées*, Vol. 10, No. 1/4, pp 5-78.

Compbell, G.S. (1974) "A simple method for determining unsaturated hydraulic conductivity from moisture retention data," *Soil Science*, Vol. 117, No. 6, pp 311-314.

Daniel, D.E., R.M. Koerner, R. Bonaparte, R.E. Landreth, D.A. Carson, and H.B. Scranton (1998) "Slope Stability of Geosynthetic Clay Liner Test Plots," *Journal of Geotechnical and Geoenvironmental Engineering*, Vol. 124, No. 7, pp 628-637.

Department of Health, Executive Yuan (1985) "Regulations for Municipal Solid Waste Landfill Facility," In: Executive Yuan Department of Health, Ed., *(2005)Wei-Shu-Fang No. 390401*.

Dho, N.Y., J.K. Koo, and S.R. Lee (2002) "Prediction of leachate level in Kimpo Metropolitan Landfill site by total water balance," *Environmental Monitoring and Assessment*, Vol. 73, pp 207-219.

Dixon, N., and D. R. V. Jones (2005) "Engineering properties of municipal solid waste," *Geotextiles and Geomembranes*, Vol. 23, No. 3, pp 205-233.

Fan, Z.X., and S.Y. Shan (2007) "In-Situ Direct Shear Test on Municipal Solid Wastes and 3-D Slope Stability Analysis," *THE 12TH CONFERENCE ON CURRENT RESEARCHES IN GEOTECHNICAL ENGINEERING IN TAIWAN*. Chi-Tou, pp C1-11-11 - C11-11-12.

Fleming, I.R., R. K. Rowe, and D.R. Cullimore (1999) "Field observations of clogging in a landfill leachate collection system," *Canada Geotechnical Journal*, Vol. 36, pp 685-707.

Foundation Conference on National Urban Cleaning (1989) "Guidebook of Final

Disposition Site of Waste."

Fungaroli, A.A., and R.L. Steiner (1979) "Investigation of Sanitary Landfill Behavior." Cincinnati, Ohio: Municipal Environmental Research Laboratory.

Giroud, J. P., and R. Bonaparte (1989) "Leakage through liner constructed with geomembrane liner--part I and II and technical note," *Geotextiles and Geomembranes*, Vol. 8(1).27-67, 8(2), 71-111, 8(4) 337-340.

ISRM (1981) *Rock Characterization Testing & Monitoring, ISRM suggested Mehods*, OXFORD: PERGAMON PRESS.

Jang, Y. S., Y. W. Kim, and S. I. Lee (2002) "Hydraulic properties and leachate level analysis of Kimpo metropolitan landfill, Korea," *Waste Management*, Vol. 22, No. 3, pp 261-267.

Kavazanjian, E. Jr., N. Matasovic, R. Bonaparte, and G.R. Schmertmann (1995) "Evaluation of MSW Properties For Seismic Analysis," *GeoEnvironment 2000*. New York,NY: Geotechnical Special Publication, ASCE, pp 1126-1141.

Klaus, B. (2000) "Validation of the hydrologic evaluation of landfill performance (HELP) model for simulating the water balance of cover systems," *Environmental Geology*, Vol. 39, No. 11, pp 1261-1274.

Koerner, R.M., and G.R. Koerner (1995a) "Leachate clogging assessment of geotextile (and soil) landfill filters, Report CR-819371," *Washington, DC: US Environmental Protection Agency*.

Koerner, R.M., and G.R. Koerner (1995b) "Leachate Clogging Assessment of Geotextile and Soil Landfill Filters." EPA/600/SR-95/141, Cincinnati, OH 45268: National Risk Management Research Laboratory.

Koerner, Robert M., and Te-Yang Soong (2000) "Leachate in landfills: the stability issues," *Geotextiles and Geomembranes*, Vol. 18, No. 5, pp 293-309.

Kuichling, E. (1889) "The relation between the raifall and the discharge of sewers in popupous districts," *Transportation Engineering, ASCE*, Vol. 20, pp 37-40.

Landva, A.O., and J.I. Clark (1990) "Geotechnics of Waste Fill," In: Arvid Landva, and Knowles G. David, Eds., *Geotechnics of Waste Fill - Theory and Practice, ASTM STP 1070*: American Society for Testing and Materials, Philadelphia, pp 86-103.

Lee, Z.H. (2008) "The Effect of Leachate Accumulation on Stability and Deformation of Solid Waste Landfills," *Institute of Civil Engineering*. Hsin-Chu: National Chiao Tung University.

Liu, C.N. (2004) "Application of Geosynthesics on Environmental Geotechnic," *Geotecnics*, Vol. 102, pp 5-14.

Mitchell, J.K., and R.B. Seed (1990) "Kettleman Hills Waste Landfill Slope Failure. I:Liner-System Properties," *Journal of Geotechnical Engineering*, Vol. 116, No.

4, pp 647-668.

Mitchell, R.A., and J.K. Mitchell (1992) "STABILITY EVALUATION OF WASTE LANDFILL," In: Raymond B. Seed, and Ross W. Boulanger, Eds., *Specialty Conference on Stability and Performance of Slopes and Embankments II (GSP 31)*. Berkeley, California: A.S.C.E., pp 1152-11187.

Mlynarek, J., and A.L. Rollin (1995) "Bacterial clogging of geotextiles: overcoming engineering concerns," pp 21–23.

Nixon, W.B., R.J. Murphy, and R.I. Stessel (1997) "An empirical approach to the performance assessment of solid waste landfills," *Waste management & research*, Vol. 15, No. 6, p 607.

Oweis, I.S., D.A. Smith, R. B. Ellwood, and D.S. Greene (1990) "Hydraulic Characteristics of Municipal Refuse," *Journal of Geotechnical Engineering*, Vol. 116, No. 4, pp 539-553.

Palmeira, E.M., A.N. Remigio, M.G. Ramos, and R.S. Bernardes (2008) "A study on biological clogging of nonwoven geotextiles under leachate flow," *Geotextiles and Geomembranes*, Vol. 26, No. 3, pp 205-219.

Payton, R.L., and P.R. Schroeder (1988) "Field Verification of HELP Model for Landfills," *Journal of Environmental Engineering*, Vol. 114, No. 2, pp 247-269.

Penman, H.L. (1963) "Vegetation and hydrology," *Technical Comment*, Vol. 53, Commonwealth Bureau of Soils, Harpenden, England.

Qian, X., and R.M. Koerner (2005) "A New Method to Analyze for, and Design against, Translational Failures of Geosynthetic Lined Landfills," *Geosynthetics and Geosynthetic-Engineered Structures, The 2005 Joint ASME/ASCE/SES Conference on Mechanics and Materials (McMat 2005)*. Baton Rouge, Louisiana, pp 61-98.

Qian, X., R.M. Koerner, and D.H. Gray (2001) *Geotechnical aspects of landfill design and construction*, Upper Saddle River, N.J.: Prentice Hall.

Richardson, C.W., and D. A. Wright (1984) *WGEN: A model for generating daily weather variables*: ARS-8, Agricultural Research Service, USDA.

Ritchie, J.T. (1972) "A model for predicting evaporation from a row crop with incomplete cover," *Water Resources Research*, Vol. 8, No. 5, pp 1204-1213.

Rowe, R.K., and J.F. VanGulck (2004) "Filtering and drainage of contaminated water," *4th International Conference on Filters and Drainage in Geotechnical and Environmental Engineering*. Stellenbosch, South Africa: Geofilters 2004.

Schroeder, P. R. , N. M. Aziz, C. M. Lloyd, and P. A. Zappi (1994a) "The Hydrologic Evaluation of Landfill Performance (HELP) Model: User's Guide for Version 3." EPA/600/R-94/168a: September 1994, U.S. Environmental Protection Agency Office of Research and Development, Washington, DC.

Schroeder, P. R. , T.S. Dozier, P. A. Zappi, B. M. McEnroe, J.W. Sjostrom, and R.L. Peyton (1994b) "The Hydrologic Evaluation of Landfill Performance (HELP) Model: Engineering Documentation for Version 3 ". EPA/600/R-94/168b: September 1994, U.S. Environmental Protection Agency Office of Research and Development, Washington, DC.

Seed, R.B., and J.K. Mitchell (1990) "Kettleman Hills Waste Landfill Slope Failure. II: Stability Analyses," *Journal of Geotechnical Engineering*, Vol. 116, No. 4, pp 669-690.

Triplett, E.J., and P.J. Fox (2001) "Shear Strength of HDPE Geomembrane/Geosynthetic Clay Liner Interfaces," *Journal of Geotechnical and Geoenvironmental Engineering*, Vol. 127, No. 6, pp 543-552.

USDA, Soil Conservation Service (1985) *National engineering handbook, section 4, hydrology*, Washington D.C.: US Government Printing Office.

USEPA (1992) "CRITERIA FOR MUNICIPAL SOLID WASTE LANDFILLS," *CFR258.40,Title 40,Design Criteria*. Washington, DC.: U.S. Gov.Print.Office.

Wang, Z.M. (2007) "Speculation of Leachate Production in MSW Landfill," *Sinotech*, Vol. 94, No. 12, pp 93-99.

ZHENG, J.M. (2004) "Studies on Slope Stabilization in Solid Waste Landfill," *MS Thesis*. Taichung County: Chaoyang University of Technology.